SANDIA REPORT

SAND96–2267 • UC–701
Unlimited Release
Printed September 1996

Screening of Hydrous Metal Oxide-Supported Catalysts for NOx Reduction by Hydrocarbons in Oxidizing Environments

Stephen E. Lott, Timothy J. Gardner, Linda I. McLaughlin

Prepared by
Sandia National Laboratories
Albuquerque, New Mexico 87185 and Livermore, California 94550
for the United States Department of Energy
under Contract DE-AC04-94AL85000

iv, 49p., excludes cover (both sides)

Issued by Sandia National Laboratories, operated for the United States Department of Energy by Sandia Corporation.

SAND 96-2267
Unlimited Release
Printed September 1996

Distribution
Category UC-701

Screening of Hydrous Metal Oxide-Supported Catalysts for NOx Reduction by Hydrocarbons in Oxidizing Environments

Stephen E. Lott
Underground Storage Technology Department

Timothy J. Gardner and Linda I. McLaughlin
Process Research Department

Sandia National Laboratories
Albuquerque, NM 87185

ABSTRACT

This report describes activities completed in August 1996 under a Cooperative Research and Development Agreement (CRADA) between Sandia National Laboratories and General Motors which began in April 1993 and was later expanded in January 1994 to include Ford and Chrysler under the Low Emission Partnership (LEP). The tasks within this effort (CRADA SC93/01155) included the evaluation of hydrous metal oxide materials as catalyst supports for the abatement of nitrogen oxides in lean-burn automotive exhaust catalyst applications.

Intentionally Left Blank

Notice

This report as a whole has conservatively been labeled as being Protected CRADA Information. This labeling, however, does not imply that the entire contents contained herein were developed as part of CRADA activities. For example, the Section entitled HMO Support Chemistry, Screening, and Selection describes materials and characterization which were completed before the initiation of CRADA activities. As such, this information is not Protected CRADA Information. The preparation of ion exchangeable hydrous metal oxide materials and general ion exchange procedures used to prepare catalyst formulations has already been previously patented by Sandia (e.g., U.S. Patent Nos. 4,511,455 and 4,929,582). However, within the scope of the current CRADA activities, some catalyst preparation procedures are, in conjunction with specific lean-burn NOx reduction catalyst or NOx adsorbent compositions, considered as Protected CRADA Information. U.S. Patent applications have been filed with respect to such materials. Protected CRADA Information in this report was formally presented to the Low Emission Partnership between October 1993 to April 1995.

Acknowledgments

The authors would like to acknowledge the technical support of the staff at General Motors, Ford, and Chrysler that ensured that this project would be a technical success. This work was performed at Sandia National Laboratories and was supported by the U.S. Department of Energy under contract number DE-AC04-94AL85000. This project was specifically supported with funds from the Technology Transfer Initiative program from DOE/DP14. Sandia National Laboratories is a U.S. Department of Energy facility.

Contents

List of Tables

List of Figures

Introduction

Lean-burn engines differ from current state-of-the-art gasoline engine technology in that the fuel is burned with an excess of air. These engines offer a potential for increased fuel economy (due to more efficient fuel combustion), reduced emissions control systems, and a lower combustion flame temperature (which should lead to increased engine life). Amendments to the U.S. Clean Air Act scheduled to be phased in over the next eight years require significantly lower emissions of nitrogen oxides (NO and NO_2, generally referred to as NOx), carbon monoxide, and total non-methane hydrocarbons, in addition to increased durability requirements for catalyst systems.[1,2,3] These pending requirements, combined with separate standards mandated to increase the corporate average fuel economy (CAFE), are pushing the U.S. automakers toward developing and marketing lean-burn engine-powered vehicles.

All gasoline-powered automobile engines require catalytic converter systems in the exhaust stream to accelerate chemical reactions which remove pollutants (NOx, CO, and residual hydrocarbons) resulting from the combustion of fossil fuels. A typical automobile catalytic converter is made of a cordierite ($2MgO{\cdot}2Al_2O_3{\cdot}5SiO_2$) ceramic material fashioned in a honeycomb design that provides a high surface area-to-volume ratio. The cordierite substrate is then coated with a washcoat, typically high surface area gamma (γ)-Al_2O_3 powder, which serves as a support for the catalyst. Next, a catalytically active material is incorporated into the washcoat. The exhaust gases passing through the honeycomb are thus exposed to the catalyst-coated surface. Typical catalyst compositions used in today's vehicles include platinum, palladium, and rhodium metals, as well as other tailored oxide additives. These catalyst systems are often referred as three-way catalysts because of their ability to simultaneously reduce NOx to N_2, oxidize CO to CO_2, and oxidize residual hydrocarbons to CO_2 and water.[2,3,4] A simple schematic showing the design and function of a typical automotive catalytic converter is shown in Figure 1.

Contemporary gasoline engines run very close to a stoichiometric air to fuel ratio (A:F=14.7±0.2) and require oxygen sensor(s) and associated air control systems. Close control of the A:F ratio is required to enable the current three-way catalyst systems to simultaneously perform the three chemical reactions described above. These conventional engine, emission control, and catalyst systems allow automobile manufacturers to meet the current U.S. Clean Air Act standards for NOx, CO, and hydrocarbon emissions. However, it is well documented that the performance of the current three-way catalyst systems is reduced significantly in oxidizing automotive exhaust environments.[1,2,3] For this reason, new catalyst systems which perform satisfactorily in oxidizing exhaust environments are required to enable lean-burn gasoline engines.

Because lean-burn gasoline and diesel engines have similar oxidizing environments, it is expected that catalyst development efforts could well exhibit significant synergism, yielding catalyst systems suitable for either application. Since the U.S. Clean Air Act has separate standards mandating significant reductions in NOx, CO, hydrocarbon, and

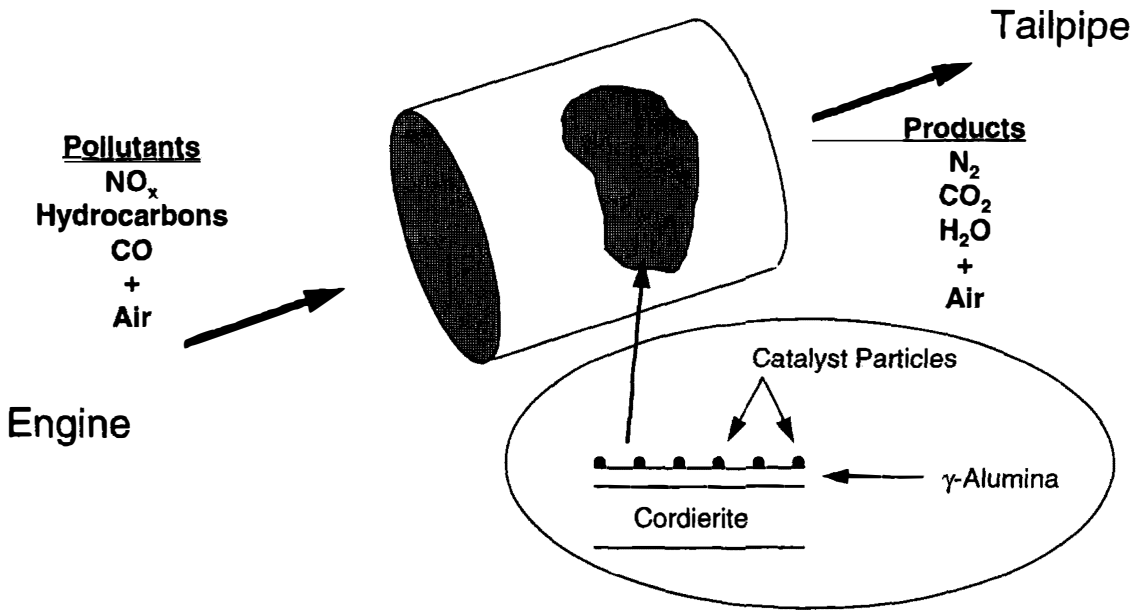

Figure 1. Schematic showing the design and function of a typical automobile catalytic converter.

particulate matter emissions over the next eight years, new catalyst systems are also required for diesel engine applications.

The overall program involved a multiple national laboratory effort; in addition to Sandia's (SNL) efforts described (in part) in this report, Lawrence Livermore National Laboratory (LLNL) evaluated aerogel-derived materials as lean-burn automotive catalyst supports, Los Alamos National Laboratory (LANL) performed fundamental studies related to zeolites and zeolite-supported catalysts, and Martin Marietta Energy Systems/Y12 Facility developed lean-burn (diesel and gasoline) engine dynamometer facilities for testing experimental full-sized catalytic converters in actual engine exhaust environments. Oak Ridge National Laboratory was also involved in CRADA activities, performing extensive catalyst characterization, mainly via eletron microscopy.

This report describes the screening procedures used to select specific hydrous metal oxide supports for evaluation, the general ion exchange and pretreatment methods used to prepare actual hydrous metal oxide (HMO) -supported metal catalysts, and catalyst activity results for a wide variety of HMO-supported metal catalysts tested using a simulated lean-burn gasoline exhaust environment in a gas phase reactor. The objective of this report is to document results from screening experiments with "bulk" catalysts. A "bulk" catalyst was defined as an active metal combined with an HMO or other conventional oxide (e.g., γ-Al_2O_3) support, with the net material existing in powder form (typically -60/+80 mesh granulated material). Screening experiments involving SNL fabricated hydrous metal oxide supports with Co, Cu, Ni, Ag, Au, Rh, Pd and Pt as active metals. A series of experiments using no catalyst or LEP-supplied catalysts (both bulk and monolith-supported forms) were performed to demonstrate proper operation of the

catalyst evaluation unit and to establish benchmarks for future catalyst activity measurements with experimental catalyst materials, respectively.

Intentionally Left Blank

Background

HMO materials were originally developed at SNL as inorganic ion exchangers for high level nuclear waste incorporation.[5] This class of materials includes hydrous titanium, zirconium, niobium, or tantalum oxides, which are chemically synthesized using sol-gel methods. Cation exchange in these HMO materials is facilitated by the manipulation of alkoxide chemistry to produce a homogeneous distribution of ion exchangeable alkali cations that provide charge compensation to the metal-oxygen framework. In terms of the major types of inorganic ion exchangers defined by Clearfield,[6] these amorphous HMO materials are similar to both hydrous oxides and layered oxide ion exchangers (e.g., alkali metal titanates).

HMO materials have many desirable characteristics for catalyst support applications, including high cation exchange capacity, anion exchange capability, high surface area, ease of adjustment of acidity and basicity, bulk or thin film preparation, and similar chemistry for preparation of various transition metal oxides. For catalyst applications, the HMO material serves as an ion exchangeable support which facilitates the uniform incorporation of catalyst precursor species. Following catalyst precursor incorporation, an activation step is required to convert the catalyst precursor to the desired active phase. Considerable previous work on HMO materials has emphasized various forms of hydrous titanium oxides as catalyst supports for direct coal liquefaction, hydrotreating, and hydrogenation/dehydrogenation applications.[7,8,9,10,11,12]

A major strength identified for the HMO materials in automotive catalyst support applications is the ability to prepare HMO-supported materials in both bulk and coated forms. Bulk catalyst preparation is typically used to rapidly screen a wide range of catalyst formulations (both different active metal and support chemistries) for catalytic activity with respect to a specific chemical reaction. The most promising catalyst materials can then be evaluated as a catalyst coating using an appropriate engineered form as a carrier. For automotive catalyst applications, the carrier of choice is a standard cordierite monolith used in automobile catalytic converters (see Figure 1). Typical monoliths, often referred to as bricks, have overall volumes, typically ranging from 110 to 150 in^3, with cell densities typically ranging from 350 to 400 cells/in^2 of cross-sectional area.

Intentionally Left Blank

HMO Support Chemistry, Screening, and Selection

Preliminary Screening

A wide variety of HMO materials have been synthesized in the past, including TiO_2, ZrO_2, Nb_2O_5, and Ta_2O_5 and various mixtures of these oxides.[10,13,14] Selection of appropriate candidate HMO support materials for automotive catalyst applications was initially based on cost, surface area, and processing experience. Due to the lack of detailed processing experience and the higher cost of niobium and tantalum alkoxides (with respect to titanium and zirconium alkoxides), hydrous niobium oxide and hydrous tantalum oxide were eliminated from the planned test matrix. This decision does not imply that these materials would not make acceptable automotive catalyst supports; it is more a reflection that the size of the actual test matrix evaluated was limited by both manpower and funds.

HMO Synthesis Chemistry

The most common systems used in previous catalyst preparation efforts at Sandia have been the hydrous titanium oxide (HTO) and hydrous zirconium oxide (HZO) systems. For both of these systems, silica doping has been used to increase the thermal stability of the supports. [9,10] These silica-doped systems are referred to by the acronyms HTO:Si and HZO:Si, respectively. The chemistry of HMO preparation has been reported in detail elsewhere,[8,9,10,15] but will be briefly summarized here for completeness. As an example, the alkoxide or sol-gel chemistry involved in the preparation of both the HTO and HTO:Si materials will be described.

HTO- or HTO:Si-supported catalyst preparation involves a multiple step chemical procedure which begins with the synthesis of a bulk HTO or HTO:Si powder. Previous work has demonstrated that SiO_2 additions (Ti:Si molar ratio = 5:1) to HTO materials act to stabilize support surface area at high temperature ($\geq$ 500°C)[9,10] without altering the ion exchange behavior.[9,16] A brief review of the synthesis of both sodium titanate (HTO) and silica-doped sodium titanate (HTO:Si) with a maximum cation exchange capacity (Na:Ti mole ratio = 0.5) will be given here as an example. In both cases, changes in the Na:Ti stoichiometry (0 < Na:Ti < 0.5) are easily accommodated. The first step of the reaction scheme involves adding the Ti (or mixed Ti-Si) alkoxide to a dilute (~10 wt.%) solution of sodium hydroxide in methanol, resulting in the production of a soluble intermediate species as follows:

$$Ti(OC_3H_7)_4 + 0.5NaOH \xrightarrow{CH_3OH} Soluble\ Intermediate \qquad (1)$$

or

$$Ti(OC_3H_7)_4 + 0.2Si(OC_2H_5)_4 + 0.5NaOH \xrightarrow{CH_3OH} Soluble\ Intermediate \qquad (2)$$

The exact chemistry involved in the formation and subsequent reaction of the soluble intermediate species is extremely complex. Possible competing reactions include

exchange of methoxide groups for isopropoxide/ethoxide groups coordinated to Ti/Si, precipitation and redissolution of titanium methoxide, partial hydrolysis or condensation of the various Si, Ti, or mixed alkoxide species, and sodium methoxide formation.[17,18,19] Under these conditions (Na:Ti=0.5), enough methanol is present to facilitate a complete exchange of all isopropoxide/ethoxide groups coordinated to Ti/Si. Structural studies completed to date indicate that the soluble intermediate is composed of a highly crosslinked Na-Ti (or Na-Ti-Si) polymer with alkoxides bridging between the various metal centers.[20]

To prepare bulk HTO or HTO:Si powders, the soluble intermediate from Equation (1) or (2) is subsequently hydrolyzed in a water/acetone solution to produce the sodium titanate or silica-doped sodium titanate as follows:

$$\textit{Soluble Intermediate} \xrightarrow{H_2O/(CH_3)_2CO} \textit{Sodium Titanate } (NaTi_2O_5H \textit{ or HTO}) \textit{ or Silica-Doped Sodium Titanate } (NaTi_2Si_{0.4}O_{5.8}H \textit{ or HTO:Si}) \quad (3)$$

The chemical formula in equation (3) assumes uniform incorporation of all reactants; this has been confirmed by various chemical analyses. The amorphous HTO or HTO:Si precipitate is filtered, washed, and vacuum dried at room temperature to produce the material for subsequent acidification/ion exchange processing.

Although similar chemistry is utilized to prepare HZO and HZO:Si supports, certain details of the chemical synthesis procedure differ significantly from HTO or HTO:Si support preparation. HZO and HZO:Si supports are prepared initially in Na form utilizing similar chemistry to that shown in equations 1 and 2, with zirconium n-propoxide used as a Zr precursor. Other differences in the chemical synthesis procedure exist with respect to the process previously described. First, the initial Zr (or mixed Zr and Si) alkoxide is added to ethanol (2:1 ratio of C_2H_5 (in ethanol):C_3H_7 (in zirconium n-propoxide) to facilitate the formation of zirconium ethoxide. The resulting solution is briefly brought to a boil, cooled to $\leq$ 50°C, and then mixed (order unimportant) with an ~10 wt.% solution of NaOH in methanol to form the soluble intermediate. Virtually no structural or chemical studies have been performed to characterize this soluble intermediate material, nor were significant attempts made to understand/improve this previously developed chemical synthesis procedure.[10] Hydrolysis of the soluble intermediate to form the bulk HZO or HZO:Si powder is very similar to that shown for the HTO or HTO:Si systems in equation 2.

Further HMO Support Screening

Following the initial down-selection, the remaining candidate HMO materials, HTO, HTO:Si, HZO, and HZO:Si, were considered for evaluation as automotive catalyst supports. All were synthesized with a Na:Ti or Na:Zr ratio of 0.5 and the silica-doped versions of these supports were evaluated at a set Ti:Si or Zr:Si molar ratio of 5:1. This

constant Ti:Si or Zr:Si ratio was set based on previous work which showed the optimum Ti:Si stoichiometry range for maximizing HTO:Si support surface area after high temperature (500°C) calcination.[9] The surface area of these four supports was evaluated as a function of calcination temperature from 100 to 1000°C using the BET method. The higher temperature limit of 1000°C was chosen based on the estimated maximum possible temperature of the catalyst surface in a catalytic converter during operation. γ-Al_2O_3, a standard catalyst support material used on cordierite monoliths (see Figure 1), is known to undergo significant surface area loss at high temperature (1000-1200°C) due to an irreversible phase transformation from γ (or other transitional form such as δ- or θ-Al_2O_3)- to α-Al_2O_3.[3,21,22]

Because surface area of the HMO materials changes significantly as Na^+ is removed from the original bulk ion exchanger, the surface area of the four HMO materials (HTO, HTO:Si, HZO, and HZO:Si) was evaluated after near complete Na^+ removal and calcination. Near complete Na^+ removal was accomplished though acidification of the original Na form of the HMO support (e.g., $NaTi_2O_5H$). After forming an aqueous slurry, H^+ ions were exchanged for Na^+ ions by adding HCl until a stable pH of 2.5 was obtained. At this pH value, well below the respective isoelectric points of each of these materials, all Na^+ was removed and no significant dissolution of the HMO occurred. These H^+ exchanged HMO materials are generally described using a shorthand notation (e.g., H^+/HTO). Previous work has shown that the surface areas of these fully acidified materials are very similar to the surface areas of metal ion exchanged materials following near complete Na^+ removal. It is desirable to remove residual Na^+ present in the catalyst precursor following ion exchange because of potential contamination problems of Na^+ in the catalyst formation.

Figure 2 compares the surface area of fully acidified HTO and HTO:Si materials as a function of calcining temperature. With the exception of the final calcination temperature, similar heating and cooling rates (nominally 5°C/min), furnace atmospheres (stagnant air), and hold times at the final calcination temperature (2 h) were used to generate the data shown in Figure 2. Very high surface areas (300-400 m^2/g) are characteristic of both the acidified HTO and HTO:Si materials in the "as-prepared" state or after low temperature (100°C) outgassing or calcination. The high surface area values associated with these as-prepared or low temperature heat treated samples represent a highly desirable feature for catalyst support applications. Moreover, it is the maintenance of appreciable surface area at elevated temperatures which is of prime importance for application of these novel materials as catalyst supports. As the H^+/HTO or H^+/HTO:Si materials are heated to higher temperatures, there is a considerable reduction in surface area, which is probably due to processes related to both crystallization of the amorphous TiO_2 material and sintering/coarsening of TiO_2 particles.

The H^+/HTO material experiences a significant reduction in surface area with increasing calcination temperature. After a 500°C/2h calcination treatment, the observed surface area of 66 m^2/g is fairly consistent with pure TiO_2 materials prepared by a variety of methods (e.g., chemical precipitation + calcining or flame hydrolysis), which typically

have surface areas ranging from 50-100 m^2/g. This calcination procedure results in a crystallization of the amorphous HTO material to form both a major anatase (JCPDS Card 21-1276) or brookite (JCPDS Card 21-1272) phase and a minor rutile phase (JCPDS Card 29-1360). Note that in weakly crystalline materials it is often difficult to distinguish the difference between the anatase and brookite phases via x-ray diffraction, since their most intense reflections have very similar d-spacings. Both of these phases have been identified at various times via either x-ray diffraction or electron diffraction in heat treated HTO- or HTO:Si-based materials. The observed crystalline phases are fairly consistent with commercial titania materials heat treated under similar conditions, although anatase and rutile are the crystalline phases usually observed in these materials.

Previous work has shown that reducing environments facilitate the conversion of anatase to rutile, both in H^+/HTO materials[23] and commercial anatase forms of TiO_2.[24,25,26] The presence of Na^+ in the HTO material can also dramatically affect the crystallographic phase evolution of HTO- or HTO:Si-based materials. Sodium titanate materials generally remain amorphous until temperatures > 600°C, where crystallization of distinct Na-Ti-O phases begins.[13] This last point further reinforces the need for ensuring near complete Na^+ removal during HTO- or HTO:Si-based catalyst preparation.

After the 500°C/2h calcination treatment, the anatase/brookite particles tend to be relatively small (20-30 nm), preserving relatively high surface areas in the H^+/HTO material. Higher temperature calcination of the H^+/HTO material results in a further significant reduction of surface area and complete conversion of the titania to well-crystallized rutile. This phase change is accompanied by a large increase in TiO_2 particle size, generally resulting in the formation of large (~0.1 μm), predominately single crystal (identified by electron diffraction) TiO_2 particles, explaining the dramatic loss of surface area.

Figure 2 also shows the results of the surface area measurements for the H^+/HTO:Si samples. These data show that the addition of SiO_2 to the HTO material has a significant effect on the physical characteristics of the support material. The surface area of the H^+/HTO:Si material after a 500°C/2h calcination was approximately double that of the H^+/HTO material after a similar heat treatment. In contrast to the H^+/HTO material, however, the x-ray diffraction results showed that the 500°C/2h calcined H^+/HTO:Si material contained only weakly crystalline anatase. Higher temperature heat treatment at 1000°C results in a further reduction in surface area to a range of 20-30 m^2/g; under these conditions the H^+/HTO:Si material has a surface area ~20x higher than the H^+/HTO material. X-ray diffraction analysis showed that the H^+/HTO:Si material calcined at 1000°C contained only anatase. These results clearly show that the addition of SiO_2 to the HTO formulation imparts increased thermal stability with respect to support surface area. The increased surface area for the HTO:Si-based samples is explained by the role of SiO_2 in retarding the anatase to rutile phase transformation at elevated temperature. This effect has been well documented in the literature, especially with similar studies related to mixed TiO_2-SiO_2 compositions.[27,28,29,30]

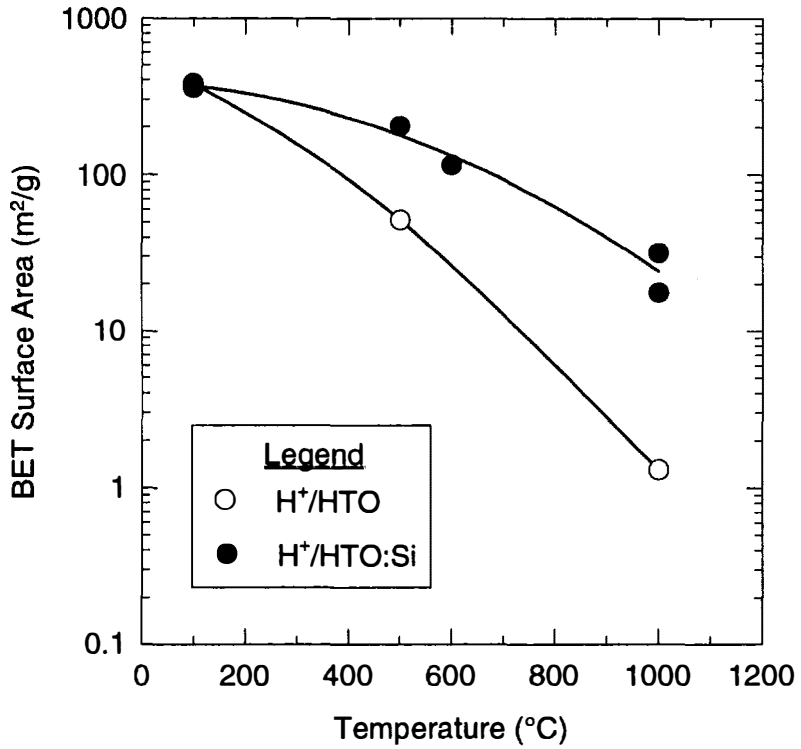

Figure 2. BET surface area as a function of calcination temperature for H^+/HTO and H^+/HTO:Si materials. Separate samples were heat treated for 2 h at the specific calcination temperature, using nominal heating and cooling rates of 5°C/min.

Figure 3 shows the results of surface area studies involving the acidified forms of HZO (H^+/HZO) and HZO:Si (H^+/HZO:Si) supports. Similar to the results obtained for the "as-prepared" or low temperature calcined (outgassed) HTO and HTO:Si supports, high surface areas, 200-300 m^2/g, were obtained after complete acidification of the Na form of the HZO and HZO:Si supports. Nearly the exact same trend was observed with increasing calcination temperature for both the HZO and HTO support materials. However, the H^+/HZO material calcined at 1000°C still had a high enough surface area (~10 m^2/g) for further consideration as an automotive catalyst support material. Similar to the case of the HTO:Si catalyst support material, SiO_2 doping was shown to produce a catalyst support material with increased thermal stability with respect to surface area. It was found that the presence of SiO_2 altered the crystallographic phase evolution of the zirconia phase; specifically, the SiO_2 was found to stabilize small particles of the tetragonal (JCPDS Card 42-1164) /cubic (JCPDS Card 27-997) phase (again, difficulty exists in the differentiation of these two phases by x-ray or electron diffraction) of ZrO_2 with respect to the large, rectangular, predominantly single crystal (identified by electron diffraction), particles of monoclinic ZrO_2 (Baddeleyite - JCPDS Card 37-1484).

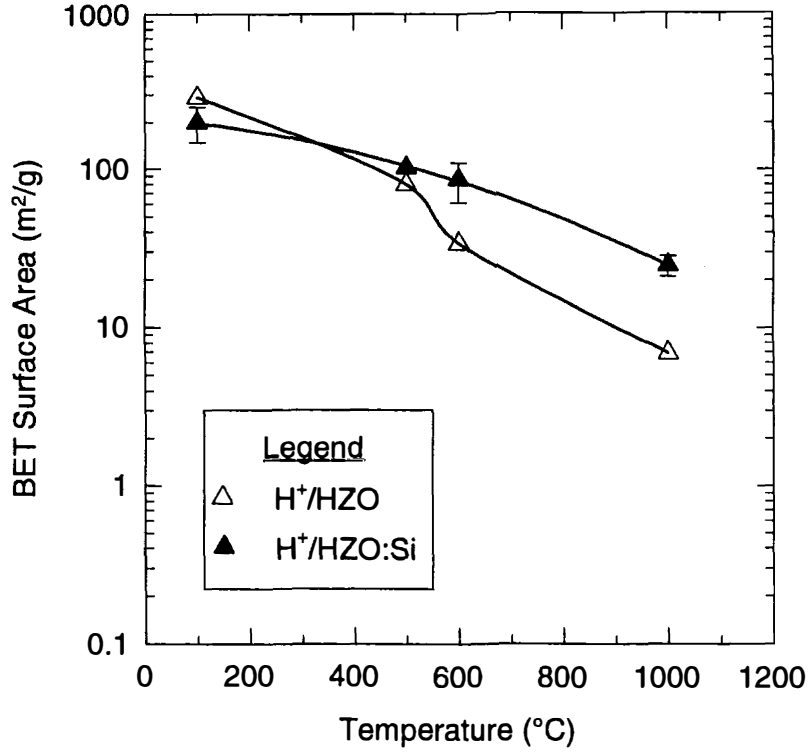

Figure 3. BET surface area as a function of calcination temperature for H^+/HZO and H^+/HZO:Si materials. Separate samples were heat treated for 2 h at the specific calcination temperature, using nominal heating and cooling rates of 5°C/min. The error bars shown indicate 95% confidence limits about the mean surface area value.

Thus, the explanation of the stabilization of catalyst support surface area for the titania- and zirconia-based systems is very similar. What is not currently known is the exact role of the SiO_2, whether it provides stabilization by surface segregation or remaining within a mixed oxide network. In the case of the TiO_2-SiO_2 system, there is no doubt that the chemical mixing typical of sol-gel processing results in the formation of Ti-O-Si bonds in the as-prepared oxide network,[31,32,33] although the actual chemical homogeneity can be influenced by many subtleties associated with the manipulation of alkoxide or other (e.g., coprecipitation) chemistry.[31,34] Phase separation would ultimately be expected to occur in the TiO_2-SiO_2 materials after heat treatment due to the fact that no solid solubility is predicted from known phase equilibria.[35] This has indeed been shown for extended high temperature (850 + 1350°C) heat treatment of TiO_2-SiO_2 glasses produced via a sol gel process, where both crystalline TiO_2 and α-cristobalite were observed.[36] A wide range of analytical techniques have been applied to the study of the structure of chemically prepared TiO_2-SiO_2 materials calcined over a range of temperatures. Nearly all studies, including those of materials produced by flame hydrolysis,[37,38,39] have shown that SiO_2 is incorporated near the surface of TiO_2 particles, stabilizing the material against sintering.[40]

Several authors have presented evidence for the existence of a titanium silicate species, or a SiO_x species significantly different from bulk SiO_2, which coats the TiO_2 particles in the case of high (> 75 mole %) TiO_2 loadings.[30,41,42] At low (< 10 wt.%) TiO_2 loadings, recent evidence indicates that it is possible that Ti^{+4} can isomorphically substitute for tetrahedrally coordinated Si^{+4} in the oxide network.[41,42]

In the case of the ZrO_2-SiO_2 system, fewer structural studies have been performed on chemically prepared samples in either the as-prepared or calcined state. Ionic size differences as well as coordination chemistry preferences would predict little substitution of Zr^{+4} into the tetrahedral SiO_2 network. Known phase equilibria suggests that a ZrO_2-SiO_2 solid solution exists for low SiO_2 loadings (< 10 mole% SiO_2), with $ZrSiO_4$ formation at high temperature for higher SiO_2 loadings (> 35 mole% SiO_2).[43] Although monoclinic ZrO_2 is the stable crystallographic phase, it is well documented that the metastable tetragonal/cubic phase can be stabilized if small particle/crystallite sizes are preserved.[44,45] Once a critical ZrO_2 particle size is exceeded, transformation to the more stable monoclinic phase occurs. As evidenced in our data, the presence of the SiO_2 apparently stabilizes the smaller ZrO_2 particles by preventing coarsening and sintering. Recent analytical studies suggest that silica is partially segregated in calcined ZrO_2-SiO_2 samples, being preferentially located at the surface of ZrO_2 particles.[46] In this sense, the role of the added SiO_2 in stabilizing high surface area is similar for both the TiO_2-SiO_2 and ZrO_2-SiO_2 systems.

The results of the support screening study therefore suggested that the most promising HMO materials for further evaluation were the HTO:Si and HZO:Si supports. Because of its fairly high temperature (1000°C) surface area stability, the HZO support was also considered for evaluation, with evaluation being limited to the most promising catalyst systems only. Except in a few cases, the HTO support was not selected for further study.

Intentionally Left Blank

Catalyst Preparation

Catalyst precursor materials were prepared using a three step procedure: ion exchange, acidification, and activation (or pretreatment). Slightly different ion exchange and acidification procedures were used depending on whether HTO or HTO:Si vs. HZO or HZO:Si supports were used. Although both cation and anion exchange are possible using HMO catalyst supports, these catalyst screening experiments all utilized cation exchange for catalyst precursor preparation. These experiments were designed to synthesize materials with nominal catalyst weight loadings of 1.0-5.0 wt.% (active metals basis after calcination). Nominal weight loadings for HMO-supported noble metal or Au catalysts were targeted at ~1.0 wt.% metal, while for the less expensive base metal or Ag catalyst systems of interest, higher metal weight loadings were targeted. Alternate ion exchange techniques and/or variations in catalyst weight loading were only considered if promising initial catalyst materials were produced via cation exchange. Development of these alternate formulations, metal weight loadings, and catalyst preparation techniques for specific systems of interest will be discussed in subsequent reports. The specific combination of metals, precursors, and HMO supports evaluated for NOx reduction activity in these screening activities are summarized in Table 1.

Table1. Matrix of active metals, salt precursors, and HMO supports evaluated.

Metal	Precursor(s)	HMO Supports
none	HNO_3	HTO:Si, HZO:Si
Co	$Co(NO_3)_2$	HTO:Si, HZO:Si
Cu	$Cu(NO_3)_2$	HTO, HTO:Si, HZO, HZO:Si
Ni	$Ni(NO_3)_2$	HTO:Si
Ag	$AgNO_3$	HTO, HTO:Si
Au	$AuCl_3$	HTO, HTO:Si
Rh	$Rh(NO_3)_3$	HTO:Si
Pd	Acidic (HCl/HNO_3) Pd Solution $Pd(NH_3)_4(NO_3)_2$	HTO:Si, HZO:Si HTO:Si
Pt	$Pt(NH_3)_4(NO_3)_2$	HTO:Si, HZO:Si

The choice of these metals was based on personal correspondences with the industrial team LEP members, success with particular metals at other National Laboratories, and promising reports in the literature.[1,47,48,49,50] For the HTO and HTO:Si supports, a straightforward and consistent cation exchange procedure was used to load a wide variety of active metal precursors. This cation exchange procedure was typically performed using a nominal batch size of 10 g HTO or HTO:Si support. First, the metal precursor salt was dissolved in 100 mL of deionized H_2O. The bulk HTO or HTO:Si support (10 g) was then added to the metal precursor salt solution. The resulting slurry was then mixed using a magnetic stir bar and stir plate. While mixing, the slurry was acidified to pH 5.5 by controlled additions of 10 wt. % HNO_3, and held at pH 5.5 for a period of 10 min, adding additional HNO_3 as necessary to control the pH. Following the conclusion of the

10 min mixing period, the solids were separated from the liquid phase by filtering using a small (100-150 mL) coarse porosity glass frit Buchner funnel.

The cation exchange procedure was followed by a second step, an acidification procedure, which was used to remove residual, unexchanged Na^+ ions from the cation-exchanged HTO or HTO:Si material. Because of the high cation exchange capacity of these materials (3-5 meq/g, 6-10 wt.% Na^+), and the relatively low metal loading targets used for these experiments, it is not surprising that significant amounts of residual Na^+ remained in the HTO or HTO:Si material after the cation exchange step. The acidification procedure was initiated by taking the residual solids captured by filtering after cation exchange and redispersing them in 100 mL of deionized H_2O. Once a suitable slurry was obtained by mixing with a stir bar and stir plate, acidification was performed by adding 10 wt.% HNO_3 to the slurry until a pH of 4 was obtained. This pH value is very close to the isoelectric point of the HTO or HTO:Si materials, where near complete H^+ for Na^+ exchange should be completed. The slurry was held at pH 4 for ~1 min, with additional HNO_3 added as necessary. A filtering procedure similar to that described above was used to separate the solids from the liquid phase. This overall acidification procedure was then repeated until the redispersed cation-exchanged HTO or HTO:Si achieved a pH of ~4 without acid addition, indicating that Na^+ removal was essentially complete. Following the final filtration step, the filtered solid was washed with acetone to remove physisorbed H_2O and facilitate drying. Following acetone washing, the remaining solids were vacuum dried under house vacuum (~3-5 in. Hg) at room temperature.

Cation exchange and acidification techniques varied slightly in the case of HZO or HZO:Si materials with respect to the HTO or HTO:Si supports. These changes were required because the HZO and HZO:Si supports were more basic than the HTO and HTO:Si materials (isoelectric point of pH 6 vs. pH 4, respectively). In these cases, an aqueous slurry of the HZO and HZO:Si support (10 g) in water (50 mL) was first prepared and acidified/stabilized at pH 8 via the addition of 10 wt. % HNO_3. Next, the metal precursor salt was dissolved in 50 mL of deionized H_2O. This metal precursor salt solution was then added to the aqueous preacidified HZO or HZO:Si-based slurry. The resulting slurry was then mixed for 30 min using a magnetic stir bar and stir plate. In the case of base metal cation exchange, the pH of this slurry was controlled below pH 7 during this mixing period to avoid potential precipitation problems. For cation exchange using noble metal ammine precursors (e.g., $Pt(NH_3)_4(NO_3)_2$), this was not necessary since these precursors are stable over a wide range of pH. Following the conclusion of the 10 min mixing period, the solids were separated from the liquid phase by filtering using a small (100-150 mL) coarse porosity glass frit Buchner funnel, washed three times with deionized H_2O and three times with acetone. Following acetone washing, the remaining solids were vacuum dried under house vacuum (~3-5 in. Hg) at room temperature. In contrast to the process used to prepare HTO- or HTO:Si-based catalyst materials, extensive acidification procedures were not usually required following the cation exchange procedure for the HZO or HZO:Si-based materials.

Use of these standard cation exchange techniques does not imply that these techniques were optimum for each metal cation of interest. It is well established that different metal cations exhibit a wide range of hydrolysis behavior in aqueous solutions.[51] This hydrolysis behavior has significant ramifications on the actual cation exchange process, since the speciation of the metal precursor species will determine the type and abundance of charged $M_x(OH)_y$ species available for cation or anion exchange. Furthermore, the cation exchange process is complicated due to: 1) the highly basic nature of the HMO materials, with the resulting solution conditions perhaps favoring precipitation of metal hydroxides rather than metal cation exchange; and 2) competition between H^+ and cationic metal precursor species for Na^+ cation exchange sites.[16]

Samples of the as-prepared catalyst precursor powders were analyzed for Na and Pt via Atomic Absorption Spectrophotometry (AAS) following dissolution of these materials (~0.5 g) in concentrated HCl. A volatiles analysis was performed on the dried catalyst precursor powder by determining the weight loss after a 600°C/2h/stagnant air calcination procedure (heating and cooling rate ~5°C/min). The AAS results were combined with the volatiles analysis results to calculate accurate metal loadings for the respective catalysts on a calcined basis.

The as-prepared HMO-based catalyst precursor powders were granulated to a size range of -60/+80 mesh. This was accomplished by first uniaxial pressing an ~2 g pellet using a 1.125 in. diameter steel die with a pressure of 12 kpsi. Light grinding with a mortar and pestle was used to generate the desired mesh fraction from the pressed pellets. Mesh fractions too fine were repressed into pellets and reground.

Granulated powder of the appropriate mesh fraction was placed in a porcelain or high purity alumina crucible or boat and calcined or "de-greened" at 600°C for 2 h (heating rate = 5°C/min) in stagnant air. In some instances, the catalysts were pretreated differently than the typical 600°C/2 h calcination step. Selected HMO-supported base or noble metal catalysts were first reduced in H_2 at 600°C for 2 h (heating rate = 5°C/min) in a quartz tube furnace, supported by quartz wool plugs. After cooling, inert purging, and passivation in 2% O_2 in N_2 at room temperature for 30 min, the catalyst samples were then calcined as described above. This reduction + calcination pretreatment procedure was used to enhance metal particle formation and prevent diffusion of metal cations into the HMO lattice. Diffusion of metal cations into the HMO lattice has been shown to be a problem in the activation of Ni/HTO catalysts.[23]

Several techniques were used to characterize the fully acidified and calcined HTO:Si (H^+/HTO:Si) and HZO:Si (H^+/HZO:Si) samples, in addition to the active metals loaded HMO-supported active metal catalyst samples. X-ray diffraction was performed at room temperature on a Siemens D-500 diffractometer with a θ-θ sample geometry and Cu K_α radiation between 2θ = 20 to 80°. Data reduction was performed using Siemens D-500 software. These x-ray analyses were performed with the knowledge that specific data regarding the crystalline state of the active catalyst phase might be impossible to obtain due to the small quantities (< 5 wt.%) of these phases. Transmission electron microscopy

was performed using a Philips CM30 instrument operating at 300 kV, with a point-to-point resolution of 0.23 nm. Sample preparation involved dispersing powder samples on Cu grids containing holey carbon films by dipping the grid directly into a mixture of the catalyst powder and butanol which had been ground using a mortar and pestle. Surface area measurements were performed on a Quantachrome Autosorb unit using the BET method.

The specific catalyst systems, metal weight loadings, and specific activation procedures evaluated in this screening study are summarized in Table 2.

Table 2. Specific catalyst compositions evaluated in this catalyst screening study.

Batch ID	Catalyst Description*	Wt.% Metal^	Wt.% Na^
LEP1-24	H^+/HTO:Si	NA	0.04
LEP1-23	H^+/HZO:Si	NA	0.03
LEP1-21	Co/HTO:Si (both RC and C)	2.07	0.40
LEP1-29	Co/HZO:Si	2.71	0.04
LEP1-22	Cu/HTO:Si	2.97	0.07
LEP1-48	Cu/HZO	2.25	0.12
LEP1-66	Cu/HZO (RC)	2.14	0.04
LEP1-47	Cu/HZO:Si (both RC and C)	2.41	0.14
LEP1-70	Ni/HZO:Si (RC)	2.32	0.29
LEP2-59	Au/HTO	1.16	0.76
LEP2-52-2	Au/HTO:Si	1.20	1.38
LEP2-54	Ag/HTO	4.03	0.05
LEP2-73-2	Ag/HTO	4.23	0.04
LEP2-46	Ag/HTO:Si	4.45	0.73
LEP1-31	Pd/HTO:Si	1.31	0.27
LEP1-61	Pd/HTO:Si	1.06	0.56
LEP1-52	Pd/HZO:Si	0.87	0.13
LEP1-32	Rh/HTO:Si	1.33	1.15
LEP1-41	Rh/HTO:Si (both RC and C)	1.02	0.09
LEP1-30	Pt/HTO:Si	1.19	0.20
LEP1-64	Pt/HZO:Si	0.77	0.11

* C denotes calcination only for the catalyst activation procedure, while RC denotes reduction followed by calcination for the catalyst activation procedure. If no designation is shown, calcination only was used for the catalyst activation procedure.

^ Metal and Na concentrations are reported on a calcined weight basis.

Catalyst Testing Procedure

The catalysts were evaluated for reduction of NOx and oxidation of propane (C_3), propylene (C_3=), and CO. A catalyst evaluation unit was designed and fabricated to blend the following gases or gas mixtures via mass flow controllers; N_2, O_2/N_2, CO_2, $CO/H_2/N_2$, NOx/N_2, and propane/propylene/N_2. Steam was added by passing the O_2/N_2 stream through a heated bubbler containing H_2O. The six gas streams were mixed via a static mixer and passed through a horizontal furnace containing the catalyst. The gas composition used for all of the experiments in this report was the following; 7% CO_2, 8% O_2, 7% H_2O, 400 ppm CO, 133 ppm H_2, 525 ppm propylene, 175 ppm propane, balance N_2. The gas streams (feed and product) were analyzed on-line with a gas chromatograph (MTI) for CO, propane, and propylene, and with a chemiluminescence analyzer (Teledyne) for NOx (total NO and NO_2).

Several different types of temperature profiles were used to evaluate the catalytic activity of the materials. "Ramp down" experiments were conducted by increasing the temperature to 500°C under N_2, passing the feed gases over the catalyst, and then lowering the temperature to a minimum of 200°C at a rate of 5°C/min or less. In some instances the catalyst was evaluated as a function of both increasing and decreasing temperature in order to identify the presence of a hysteresis phenomenon, indicative of adsorption/desorption. For this "ramp up/ramp down" mode, the furnace was first held at 150°C for 20 min, ramped to 500°C at 5°C/min, held at 500°C for 30 min, and then cooled to at least 200°C at a rate of 5°C/min or less. During the evaluation of some of the Cu catalysts (Cu/ZSM-5 and Cu/HMO), the maximum temperature was 600°C as opposed to 500°C due to the higher light-off temperature of these materials. Typically, NOx readings were taken every 30 seconds, while gas chromatograph injections were taken every 5 min. For some materials, the degree of adsorption / desorption hysteresis was significant, therefore, isothermal measurements were made of the catalytic activity. Isothermal catalyst activity measurements were taken by holding the temperature constant for a minimum of 30 min until the measured concentration of CO, propane, and propylene from the on-line gas chromatograph and NOx from the chemiluminescence analyzer was constant. Upon completion of an isothermal activity measurement, the temperature was stepped to the next desired temperature. Isothermal activity measurements can be easily differentiated from "ramp-up" or "ramp-down" activity measurements by noting the fewer number of data points in the activity profile. For both sweep and isothermal measurements, all catalyst activity testing concluded with re-evaluating the feed gas composition to ensure that the gas chromatograph and the a chemiluminescence analyzer calibrations were still valid.

In the case of the zeolite-supported commercial catalysts, steam ageing experiments were also performed to monitor their stability. For these experiments, the initial (fresh) activity of a cordierite monolith-supported catalyst was measured in the catalyst evaluation unit. The catalyst was then transferred from the catalyst evaluation unit to a steam ageing unit, consisting of a separate quartz tube furnace. Ageing experiments were performed for extended periods (~1 week) at 650°C in an 8% steam, balance air, atmosphere.

Following this ageing treatment, the catalyst was removed and retested in the catalyst evaluation unit to determine the degradation in performance. These ageing experiments were performed to compare activities with zeolite-supported metal catalysts which have been shown to exhibit significant degradation of activity in steam environments.[52,53,54,55] This was one reason for surveying a number of alternate, non-zeolite support materials under the scope of this multi-laboratory CRADA effort.

In addition to the screening tests, a series of baseline runs were made to determine whether the catalyst evaluation unit was operating properly. These experiments included evaluating LEP furnished materials and performing blank run experiments.

In most instances, the bulk materials were evaluated at 20,000 scc feed gas per h per cc of catalyst material, equivalently expressed as 20,000 1/h or 20 k/h. Approximately 1.5 g of granulated and pretreated material was supported in a 13 mm ID quartz reactor tube with quartz wool plugs.

In most instances, the monolith supported materials were evaluated at 50,000 scc feed gas per h per cc of monolith, equivalently expressed as 50,000 1/h or 50 k/h. Small monolith cores (13 mm in dia and 10 mm length) were cut from full sized monoliths (85 in^3 or 110 in^3). A typical sample had a volume of 1.33 cm^3 and required a flow rate of 1108 sccm. Partial cells on the edge of the monolith that did not contact the quartz tube were filled by sealing with small pieces of quartz filter paper.

Results of Flow Reactor Experiments

A summary of the screening experiments pertinent to this report is detailed in Appendix 1. Specific catalyst screening experiments are reviewed in the following sections: Baseline Screening Evaluation, HMO-Supported Base Metal Catalysts, HMO-Supported Gold and Silver Catalysts, and HMO-Supported Noble Metal Catalysts. Results are expressed in terms of maximum percentage conversion of NOx, CO, propylene, or propane and the temperature at which the maximum percentage conversion occurred. The number shown in parentheses indicates the experiment number, which along with the Batch ID from Table 2 can be used to cross-reference these results to those reported in Appendix 1.

Baseline Screening Evaluation

Homogeneous Gas Phase Reactions

To determine the extent of homogeneous reactions, a blank run (#187) was made with an open 13mm ID quartz tube to identify the magnitude of gas phase reactions that occur as a function of temperature. The flow rate was set at 50 k/h assuming a 1 cm length catalyst bed. Little NOx reduction was detected over the entire temperature range; a maximum of 8% conversion was observed at 500°C. At this temperature, CO, propylene, and propane conversions due to gas phase reactions were -15, 14, and 23%, respectively. The negative conversion of CO to CO_2 indicated that more CO was produced from the oxidation of the propane and propylene than was oxidized to CO_2. Similar observations have been seen by other researchers on the LEP team.

To compare with the results of the open quartz tube, runs were also made with a $NaTi_2O_5H$:0.4SiO_2-coated alumina/cordierite monolith section. Although the Na form of the catalyst was used, the purpose of these monolith runs was to furnish a gas heating medium, thus to ensure that the gases in the quartz tube were heated to the furnace temperature. The runs were performed with both the standard feed mixture (#188/#189) and with NO_2 substituted for NO (#190/#191). The space velocity was 50 k/h for all four runs. For the runs with the NO feed, at 503°C only 6% of the NO was reduced indicating that the $NaTi_2O_5H$:0.4SiO_2-coated alumina/cordierite monolith had little effect on NO reduction, with the results being very similar to the open tube runs. The oxidation activity of the $NaTi_2O_5H$:0.4SiO_2-coated alumina/cordierite monolith was also very similar to the open quartz tube run, with CO, propylene, and propane conversions of -4, 14, and 7% respectively. For the NO_2 feed, the NO_2 adsorbed and desorbed, making quantification of actual catalytic activity impossible. However during the isothermal portion of the temperature profile at 500°C, little catalytic NO_2 reduction occurred. At 500°C oxidation of CO, propylene, and propane with the NO_2 feed was also low; -8%, 9%, and 1% respectively.

Bulk Washcoat Powders Supplied by General Motors

Baseline runs of washcoat powders were made with DSZ-5b, a Cu/ZSM-5 material (#89) and Tech-3 (#90). The DSZ-5b formulation consisted of 4.5 wt.% Cu supported in a

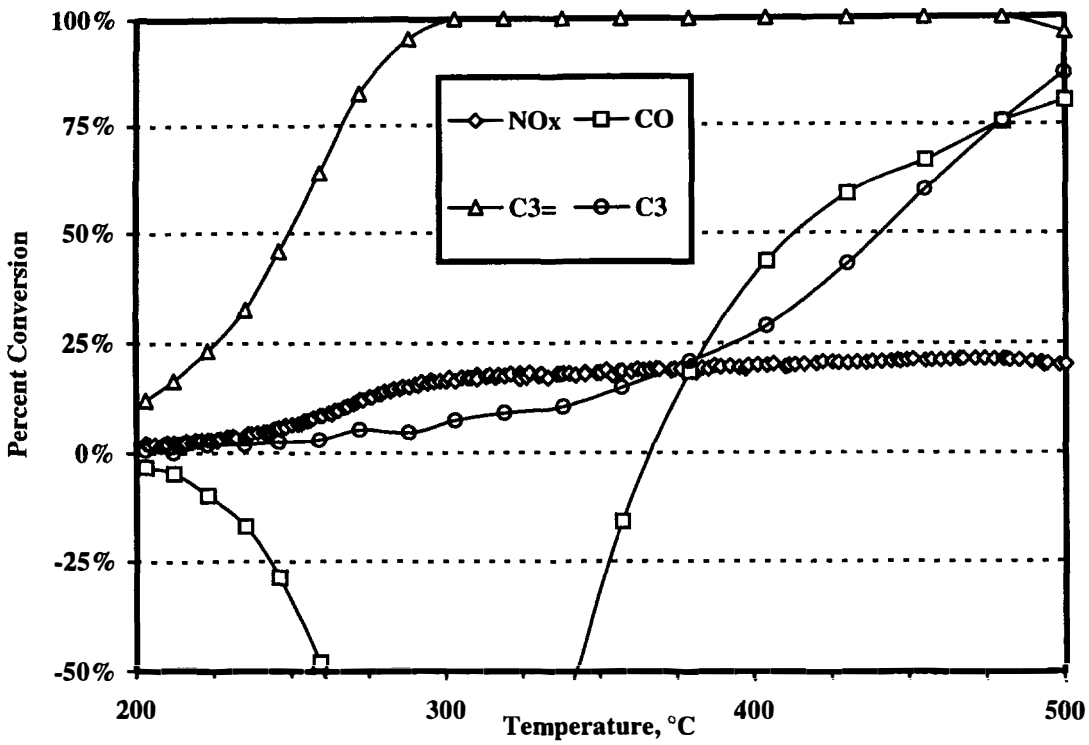

Figure 4. Activity of GM supplied DSZ-5b washcoat at 20,000 1/h.

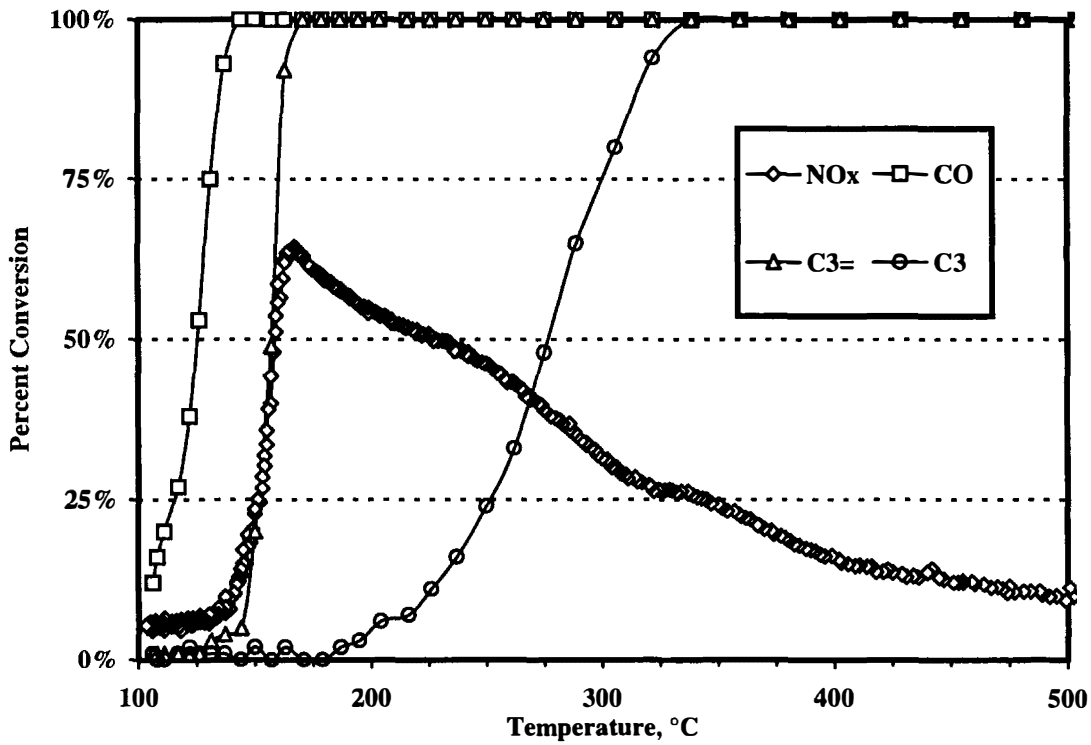

Figure 5. Activity of GM supplied Tech-3 washcoat at 20,000 1/h.

ZSM-5 zeolite matrix, while Tech-3 was a GM/Delphi proprietary washcoat formulation for lean-burn operation containing precious metals; the Tech-3 powder material contained 0.426 wt.% Pt and 0.043 wt.% Rh. Monoliths that had the washcoat applied for both the DSZ-5b and the Tech-3 were also evaluated (see next section). NOx, CO, propane, and propylene activity for the two washcoat powders are shown in Figures 4 and 5.

The DSZ-5b washcoat powder had a broad NOx conversion at 20 k/h with a maximum value of 24% at 480°C (#89/#91). Note the higher number density of data points for the NOx conversion data due to the higher sampling frequency. The propane and propylene oxidation profiles were typical of Cu materials evaluated under this CRADA and by other investigators.[56,57] Also typical was the CO oxidation activity, illustrating that more CO was produced from the oxidation of propane and propylene than could be oxidized to CO_2. At 20 k/h the Tech-3 washcoat powder had a maximum NOx conversion of 63% at 171°C. Oxidation of propane, propylene, and CO was very good and typical of a Pt catalyst.[58,59,60]

Cordierite Monolith-Supported Catalysts from General Motors and Commercial Catalyst Suppliers

For the DSZ-5b material, the Cu loading was 4.5 wt.% in the zeolite and 40 wt.% of the washcoat was zeolite; therefore the washcoat contained 1.8% Cu. The washcoat loading was 200 g per L of monolith volume. The DSZ-5b monolith was run at a space velocity of 20 k/h under two conditions; with and without steam. These reaction profiles will not be shown, with only a word description of the results. In the presence of steam, the NOx conversion was 12% (#48) at 500°C. The CO concentration increased as propylene was oxidized and never was reduced below the feed concentration. The propylene was not fully oxidized at 400°C. Only 12% of the propane was oxidized at 500°C. A fresh as-received monolith sample was run without steam in the feed gas and the NOx conversion increased to 29% (#47) at 500°C. The oxidation behavior slightly improved with the removal of the steam. The propylene was fully oxidized at temperatures over 370°C and 66% of the propane was oxidized at 500°C. This data illustrates that steam has significant short-term effects on the activity of Cu/ZSM-5 catalysts in addition to the well established long-term degradation of catalyst performance. Additional experiments would be required to determine the potential reversibility[52] of these short-term effects and if steam altered the mechanism of NOx reduction over Cu/ZSM-5 catalysts.

For the Tech-3 material, the washcoat loading was 3.25 g per in^3 on the supplied 85 in^3 brick. The precious metal loading of Pt and Rh was 0.038 troy oz and 0.0038 troy oz respectively on a brick basis. The NOx conversion activity was tested at space velocities of 20 k/h and 50 k/h (#4 and #2 respectively). The NOx activity profiles are shown in Figure 6.

The NOx reduction activity was 74% (#4) and 46% (#2) at space velocities of 20 k/h and 50 k/h, respectively. As to be expected, the peak NOx reduction activity was higher for the lower space velocity; however, at the higher space velocity, appreciable NOx

reduction occurred at higher temperature, and was extended over a broader temperature range.

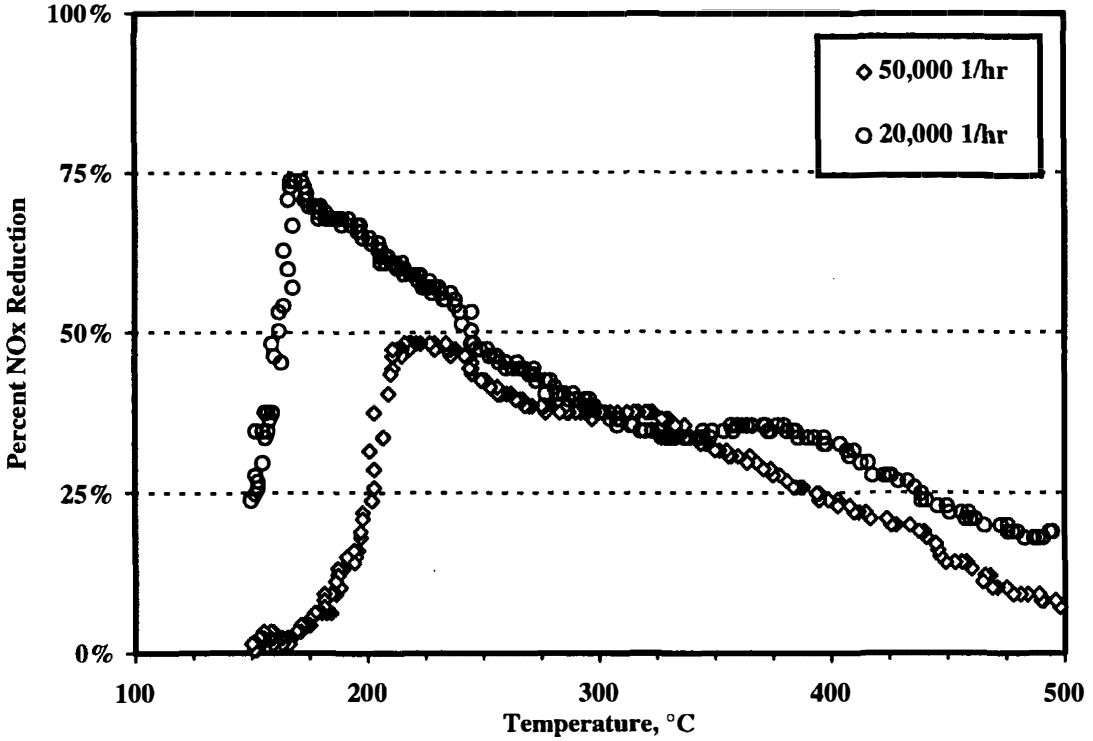

Figure 6. NOx reduction activity of GM supplied Tech-3 monolith.

A series of experiments were run at 50 k/h with Pt/ZSM-5 and Cu/ZSM-5 powders (washcoats) supported on cordierite monoliths supplied by Johnson-Matthey. The active metal weight loading on a washcoat basis for the Pt/ZSM-5 and the Cu/ZSM-5 was 1.09% and 3.0% respectively. The washcoat loading was 200 g per L of monolith and the density of the Pt/ZSM-5 and the Cu/ZSM-5 monoliths were 927 g and 890 g per 110 in^3. Thus the loadings on a total brick weight basis were 0.42% and 1.22% for the Pt/ZSM-5 and the Cu/ZSM-5 monoliths respectively.

Four experiments to evaluate the NOx reduction activity were made with the Cu/ZSM-5 monolith supported catalyst for the following conditions; as-received or calcined at 600°C for 2 h, and with or without steam in the simulated exhaust gas mix (#237-#240). All runs were made with a temperature sweep from 150°C to 600°C to 150°C at a rate of 5°C/min. In general, calcination may have slightly increased the Cu/ZSM-5 NOx reduction activity. The addition of steam did not have a deleterious effect in the short term; experimental results were similar between runs with and without steam. The maximum NOx conversion for the four runs ranged from 52% to 69%. The isothermal catalytic activity profile for the run with steam and calcination is shown in Figure 7. As with other Cu materials, the CO oxidation activity is poor. The CO profile has two increases in concentration (negative conversion); when the propylene and the propane are significantly oxidized at ~350°C and ~525°C, respectively.

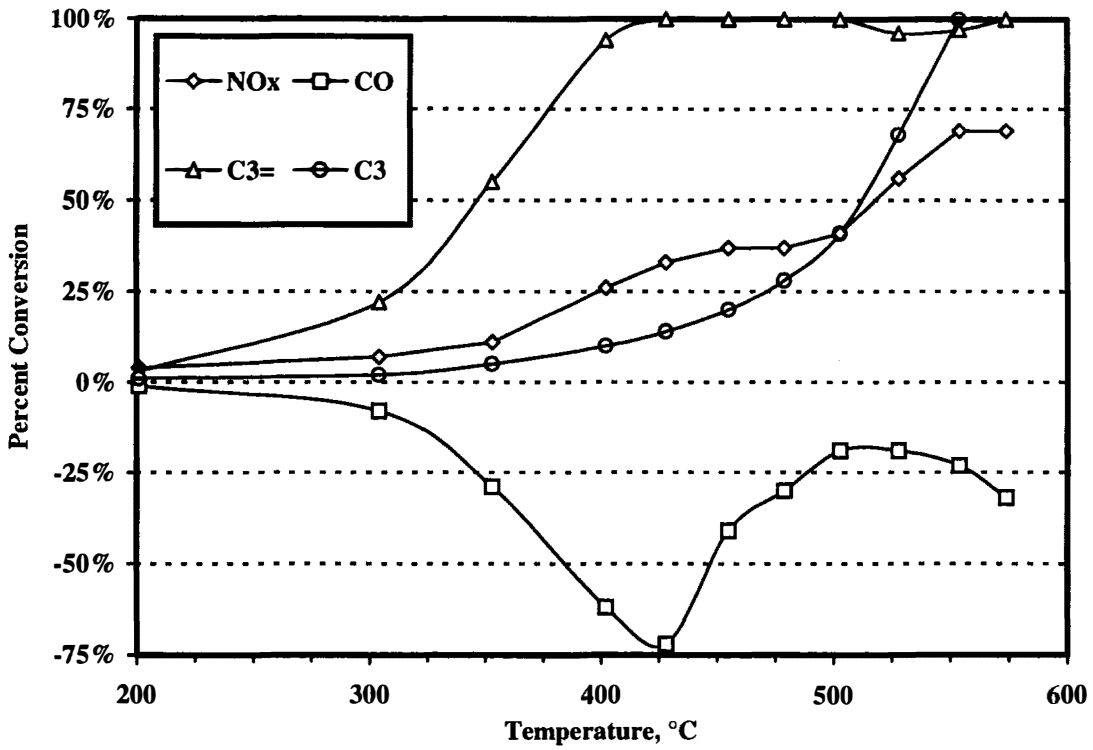

Figure 7. Isothermal activity of Johnson Matthey supplied Cu/ZSM-5 monolith at 50,000 1/h.

An attempt was made to determine the impact of steam ageing on the catalyst performance since it is well recognized that this can result in significant degradation of Cu/ZSM-5 catalyst activity.[52,53,54] After 1 week ageing at 650°C in 7% steam, balance air, the catalyst performance almost completely degraded. The maximum NOx reduction activity was only 9% and CO oxidation performance was very poor; -160% conversion at 568°C (#309).

For the Pt/ZSM-5 catalyst, the same series of runs were made as in the case of Cu/ZSM-5. All runs were made with a temperature sweep from 150°C to 500°C to 150°C at a rate of 5°C/min. Of the four runs comparing the effect of steam/no steam and calcination/as-received, no clear effect of either calcination or steam was noted (#232/#233/#235/#236). The NOx reduction for the four runs ranged from 37% to 54%. Run #235 for the calcination and with steam case is shown in Figure 8; maximum NOx conversion is 37% at 354°C. The NOx profile is desirably flat with a wide temperature window. After 1 week ageing in air and 7% steam at 650°C (#262/#298), the activity dropped to 28% at 380°C (Figure 9 for run #298). All catalyst activity was impacted with the propane oxidation and the NOx reduction most severely reduced.

In summation, the blank runs (no catalyst or only cordierite) were truly blank runs with little or no apparent NOx reduction. The Cu/ZSM-5 catalysts were reasonably active, however, catalytic activity was significantly lower after steam ageing (>80% decreased). Approximately 1/3 of the Pt/ZSM-5 activity was lost with steam ageing. The

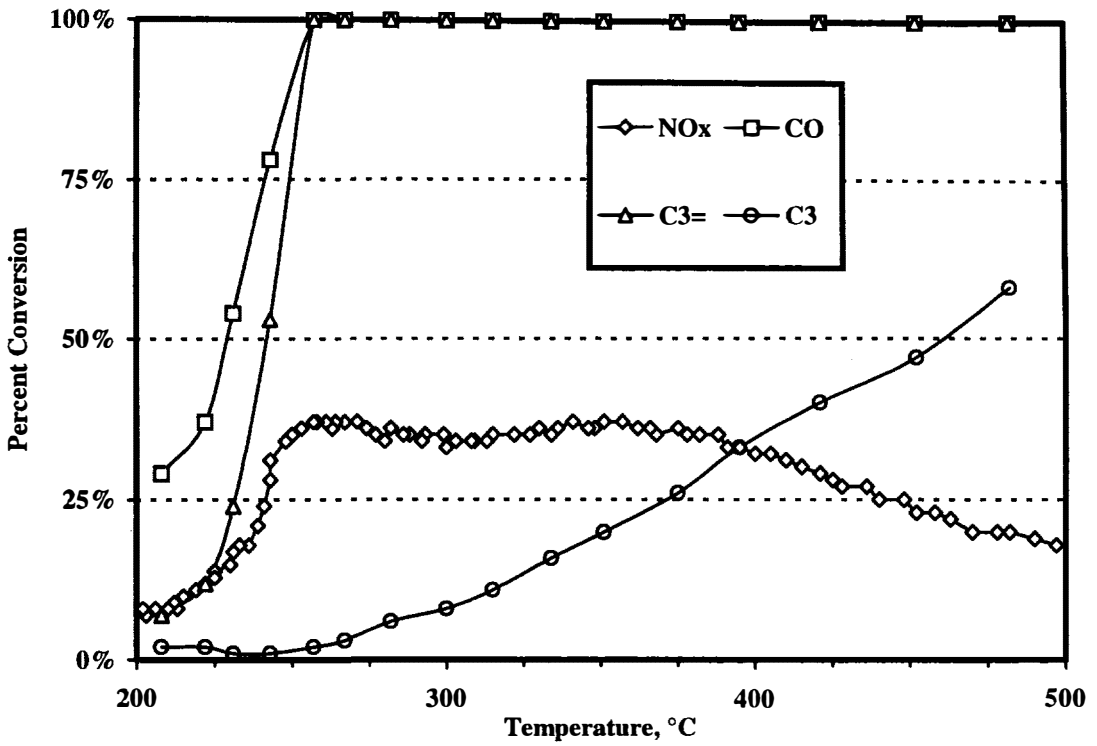

Figure 8. Activity of Johnson Matthey supplied Pt/ZSM-5 monolith at 50,000 1/h.

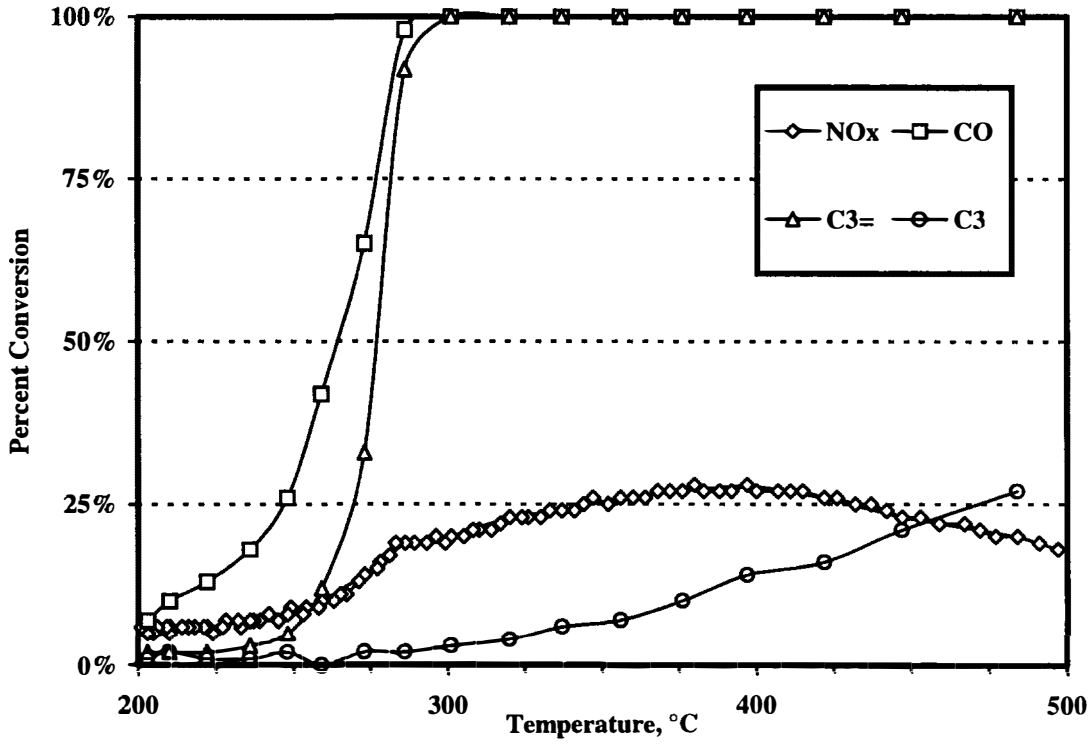

Figure 9. Activity of Johnson Matthey supplied Pt/ZSM-5 monolith at 50,000 1/h after steam ageing.

performance of the Pt/ZSM-5 catalyst in the steam ageing environment was consistent with at least one published report in the literature stating that Pt/ZSM-5 catalysts showed a significant resistance to deactivation with respect to H_2O and SO_2 tolerance compared to Cu/ZSM-5 catalysts.[61] Although this report[61] did not specify ageing conditions, aggressive ageing conditions (700-800°C in steam) resulted in a total loss of catalyst activity for Pt/ZSM-5 in a separate study.[55]

Bulk H^+/HTO:Si and H^+/HZO:Si Powders

Screening experiments were made with two of the baseline support materials, HTO:Si and HZO:Si. As previously discussed, these materials were prepared in an acidified form, resulting in near complete removal of Na^+ (see Table 2). These acidified forms were therefore representative of the baseline support materials present in a HTO:Si- or HZO:Si-supported metal catalyst with low Na^+ content (see Table 2). The H^+/HTO:Si material was evaluated at two different space velocity conditions: 20 k/h (#9) and 50 k/h (#6). The maximum NOx reduction for these two flow conditions occurred at 500°C, being 16% and 10%, respectively. Negligible NOx conversion occurred for either run at a temperature less than 450°C (see Figure 10 for 20 k/h data). At 20 k/h and 500°C, the oxidation behavior of this sample was poor; conversions of -48%, 76%, and 24% were observed for CO, propylene, and propane, respectively. As previously described in the section on Further HMO Support Screening, this sample showed the presence of weakly crystalline anatase/brookite following the 600°C calcination procedure.

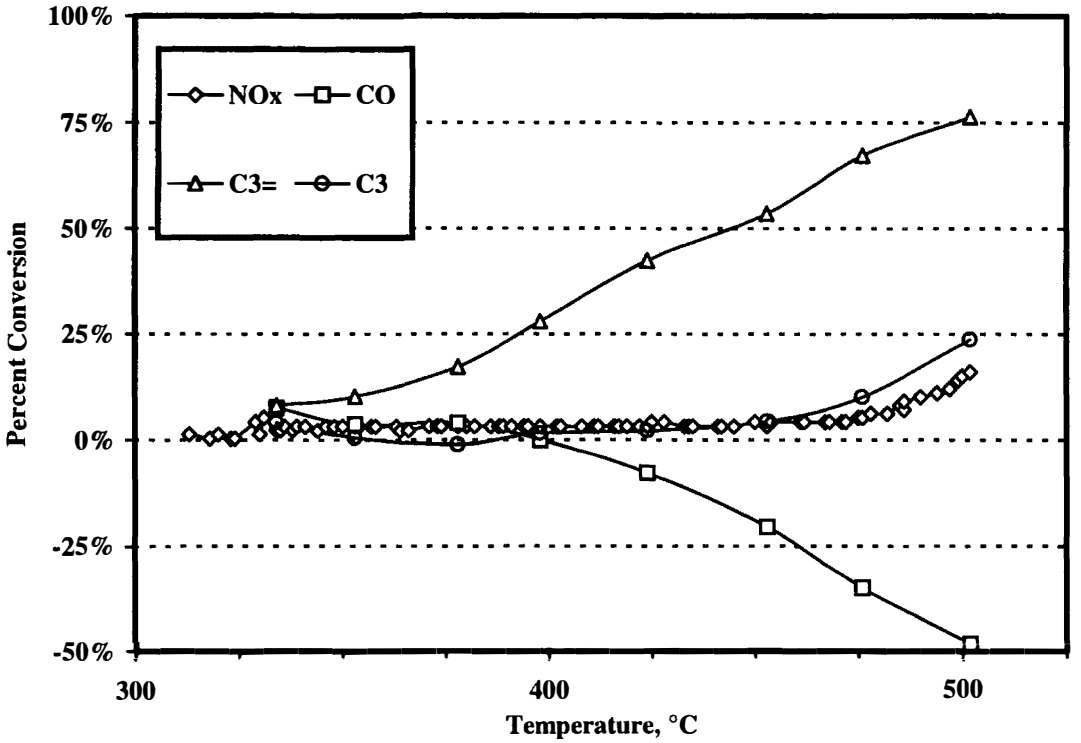

Figure 10. Activity of H^+/HTO:Si powder at 20,000 1/h.

The NOx reduction behavior was less than 2% for both the H^+/HTO:Si material and open quartz tube at temperatures < 450°C. Only above 450°C did the H^+/HTO:Si material

differentiate itself from the open quartz tube experiment. At 500°C, 10% of the NOx was reduced with the H^+/HTO:Si, while at 500°C, 3% of the NOx was reduced in the open quartz tube. The propane oxidation activity was similar for the two experiments. The propylene oxidation rate for the H^+/HTO:Si material was poor (11% conversion at 400°C), however, the rate was higher than the negligible rate with the open quartz tube. The propylene oxidation activity for the H^+/HTO:Si material caused negative CO oxidation rates, i.e., more CO was produced than could be oxidized.

Similar experiments were performed with the acidified HZO:Si (H^+/HZO:Si) material (see Table 2). At space velocities of 20 k/h (#11) and 50 k/h (#7), the NOx reduction was negligible, being less than 5% up to 500°C. At 20 k/h and 500°C, the oxidation behavior was better than the HTO:Si support; conversions of 73%, 100%, and 20% for observed for CO, propylene, and propane, respectively (Figure 11). As previously described in the section on Further HMO Support Screening, this sample showed the presence of weakly crystalline tetragonal/cubic zirconia following the 600°C calcination procedure.

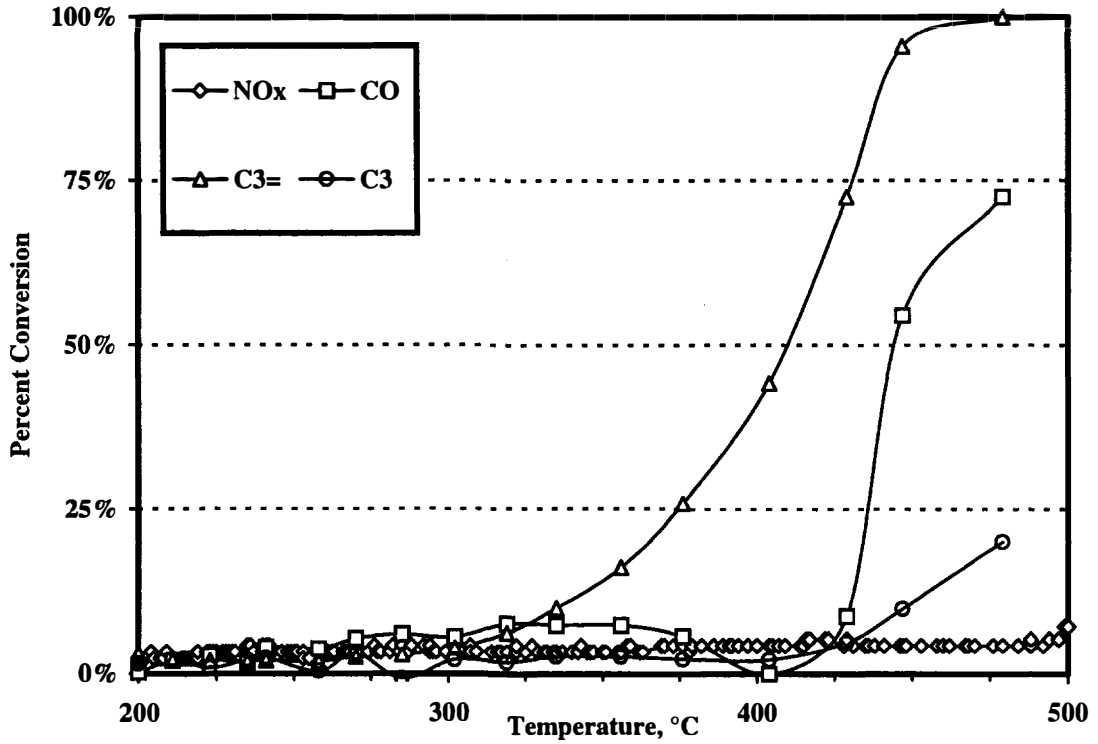

Figure 11. Activity of H^+/HZO:Si powder at 20,000 1/h.

In summary, the H^+/HTO:Si and the H^+/HZO:Si base supports displayed little NOx reduction activity below 450°C. The H^+/HZO:Si support displayed moderately better oxidation behavior than the H^+/HTO:Si support indicated by the higher propylene and CO oxidation rates. This result is possibly related to the higher acidity of ZrO_2-SiO_2 mixed oxide materials versus TiO_2-SiO_2 mixed oxide materials.[34,62] Based on these results, little contribution of the support materials would be expected in the case of HMO-supported metal catalysts used for NOx reduction applications.

HMO-Supported Base Metal Catalysts

Due to the constraints of time and funding, the screening study was confined to investigating only a few base metals. Co, Ni, and Cu were selected based on success in the literature by other researchers studying non-HMO supports (e.g., alumina and zeolites).[1,47,48,49,63]

Evaluation of Bulk Co/HTO:Si and Co/HZO:Si

A 2.07% Co/HTO:Si material was prepared, calcined at 600°C, and evaluated at space velocities of 20 and 50 k/h (#13 and #8, respectively). This material was a poor NOx reduction catalyst. The maximum NOx conversion at either 20 or 50 k/h was less than 5%, which was lower than the baseline H^+/HTO:Si material, with the temperature of maximum conversion near the maximum sweep temperature (500 and 506°C, respectively). The oxidation behavior of this catalyst was also poor. The conversion of CO, propylene, and propane were 12%, 94%, and 22% at 20 k/h (500°C) and -62%, 42%, and 4% at 50 k/h (506°C). X-ray diffraction analysis of the catalyst after calcination showed the existence of weakly crystalline brookite/anatase, being very similar to the results obtained for the H^+/HTO:Si support calcined under similar conditions.

To investigate the effect of a different catalyst activation treatment, part of the 2.07% Co/HTO:Si material was reduced prior to calcination using the procedure previously described; 600°C for 2 h under H_2, cooled to room temperature under H_2, inert gas purging at room temperature, passivation under 2% O_2 in N_2 for 30 min at room temperature, followed by calcination at 600°C for 2 h. The purpose of this alternate pretreatment procedure was to form metallic Co particles prior to calcination so as to inhibit diffusion of Co^{+2} ions into the amorphous HTO:Si structure during the calcination treatment. However, the resulting catalyst did not perform significantly different from the Co/HTO:Si catalyst which was pretreated using only the standard calcination procedure only. The maximum NOx conversion observed for this catalyst was only 5% (#56).

A 2.71% Co/HZO:Si material was prepared, calcined at 600°C, and tested at 20 k/h (#15). While the maximum NOx conversion of 13% (432°C) was an improvement over the Co/HTO:Si material, oxidation behavior remained poor; -47%, 81%, and 30% for CO, propylene, and propane. After calcination, this material was observed to be x-ray amorphous.

In summary, Co/HMO:Si materials performed slightly better than the base supports (H^+/HTO:Si and H^+/HZO:Si), however, the catalytic enhancement of Co was not remarkable. In addition, oxidation behavior remained poor, illustrated by the poor CO oxidation rates.

Evaluation of Bulk Ni/HZO:Si

One batch of 2.32% Ni/HZO:Si was prepared and pretreated using only the reduction and calcination procedure and then tested at 20 k/h (#57). This catalyst had low NOx reduction activity (less than 10% conversion at 367°C) and fairly low oxidation activity

(75% CO conversion, 70% propylene conversion, and 6% propane conversion). No additional Ni/HMO materials were evaluated.

Evaluation of Bulk Cu/HMO Materials

Since zeolite- and oxide-supported Cu catalysts had been shown to have high activity for NOx reduction in oxidizing environments,[1,47,48,49] we chose to evaluate Cu supported on three of the four of the candidate hydrous metal oxide supports (HTO:Si, HZO, and HZO:Si).

Bulk Cu/HTO:Si

A 2.97% Cu/HTO:Si material was prepared and evaluated after calcination at 600°C. Samples from this batch were tested at both 20 k/h (#12) and 50 k/h (#14); maximum NOx conversion was only 10% (254°C) and 6% (272°C), respectively. At the lower space velocity, conversion for the oxidation reactions was 59%, 93%, and 2% for CO, propylene, and propane, respectively. X-ray diffraction results for the calcined material showed the existence of only weakly crystalline anatase/brookite.

Bulk Cu/HZO and Cu/HZO:Si

One Cu/HZO:Si and two Cu/HZO materials were prepared for screening. Separate Cu/HZO batches were required to test the effects of the various catalyst pretreatment procedures (calcination only vs. reduction + calcination). Batch preparations are generally very reproducible in terms of catalyst performance, so this experiment allowed a fair experiment involving the effect of the pretreatment procedure. In contrast, a single batch of Cu/HZO:Si material was pretreated using both techniques and tested.

For the Cu/HZO results, the pretreatment procedure was found to have little effect on the catalyst performance (Figure 12), although the reduced and calcined (RC) material exhibited a light-off temperature about 25°C lower than the calcined (C) material. For both materials, the CO oxidation was 100% for temperatures greater than 200°C. For the calcination pretreatment (#33), a maximum NOx conversion of 14% was observed at 393°C, while a corresponding value of 17% was observed at 378°C for the reduction + calcination pretreatment procedure (#51).

The Cu/HZO:Si material produced very interesting results which indicated an apparently important catalyst pretreatment effect. The standard calcination procedure (#34) produced a material which performed similar to the Cu/HZO materials described above. Maximum NOx conversion was 15% at 307°C. However, the reduction + calcination pretreatment (#45) resulted in a significant improvement in catalyst performance. NOx conversion showed a steady improvement with increasing temperature, exhibiting a maximum of 92% at 500°C. Figure 13 shows the NOx conversion plots along with the oxidation activities for CO, propylene, and propane for the calcined (C) and reduced and calcined (RC) pretreatments. For the reduced and calcined pretreatment, all of the oxidation activities were retarded to higher temperatures.

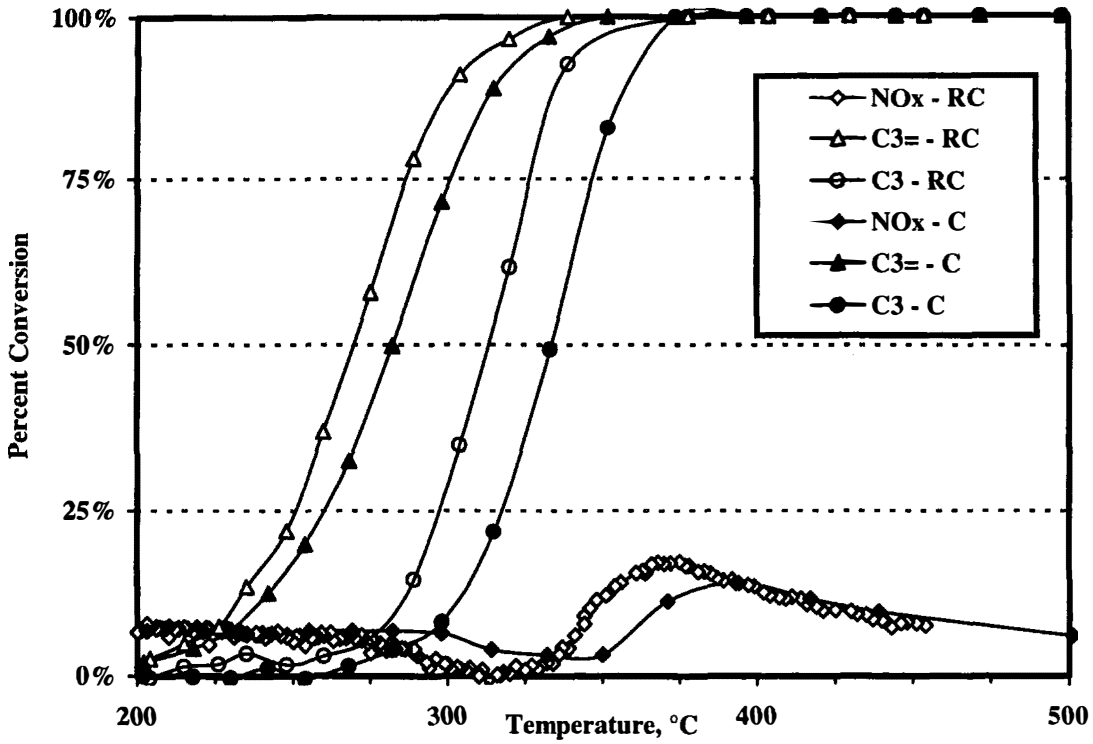

Figure 12. Effect of pretreatment of Cu/HZO powder at 20,000 1/h

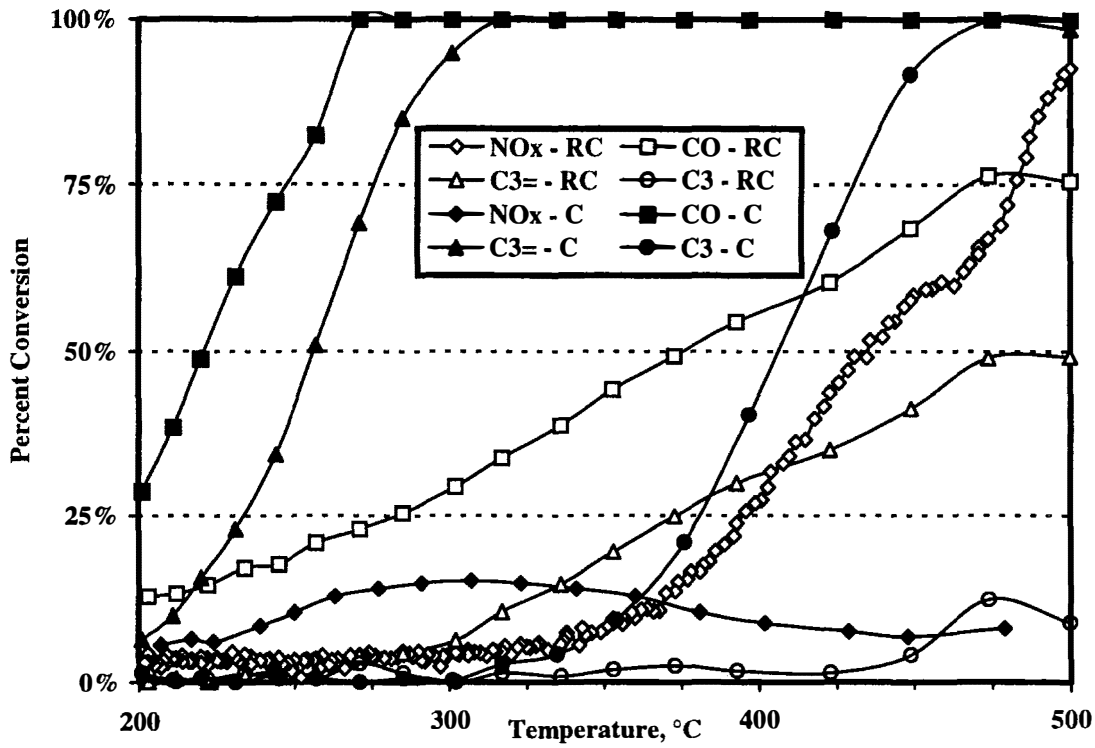

Figure 13. Effect of pretreatment of Cu/HZO:Si powder at 20,000 1/h.

To verify these results, this same sample was later reloaded into the reactor and retested (#50). This retest yielded a maximum NOx conversion of 40% at 465°C. Although not perfectly reproducible, both of these results generated significant interest in this material for NOx reduction applications.

X-ray diffraction analysis of the Cu/HZO and Cu/HZO:Si materials was performed as part of the initial qualitative catalyst characterization efforts. After calcining only, the Cu/HZO material was found to contain both weakly crystalline tetragonal/cubic (major phase) and monoclinic (minor phase) ZrO_2. No significant difference in crystalline phase content was found for the alternate reduction + calcination pretreatment. These results were consistent with those obtained for the acidified HZO (H^+/HZO) support material reported earlier. These similar x-ray diffraction results were also consistent with the fact that the catalyst activity results were also very similar for either pretreatment procedure.

In contrast, the x-ray diffraction results for the Cu/HZO:Si as a function of catalyst pretreatment were very interesting. After calcining only, the Cu/HZO:Si material contained only weakly crystalline tetragonal/cubic ZrO_2. However, the x-ray diffraction results for the reduced + calcined material (LEP1-47) were significantly different. These results indicated the presence of CuO (tenorite) and sodium zirconium silicate (Na_2ZrSiO_5) in addition to the weakly crystalline tetragonal/cubic ZrO_2 phase. These results were surprising in that two unique phases, CuO and Na_2ZrSiO_5, were identified in the reduced + calcined material but not in the calcined only material. In particular, the presence of the Na_2ZrSiO_5 phase was surprising since the initial elemental analysis of the as-prepared batch (LEP1-47) showed a very low Na^+ level (see Table 2). This finding suggests the possibility of significant Na^+ contamination of this catalyst sample, with the contamination being introduced <u>after</u> catalyst preparation (i.e., during the granulation, pretreatment, or testing steps). Since two new unique phases were identified by x-ray diffraction in the case of this material, it could not be straightforwardly determined which specific phase(s) (if any) were directly responsible for the improved performance of this reduced + calcined Cu/HZO:Si material. The x-ray diffraction results for this sample were also confirmed by performing electron diffraction measurements in conjunction with transmission electron microscopy.

Upon further investigation, it was found that the reduced + calcined Cu/HZO:Si material was a <u>strong adsorber of NO and not a catalyst.</u> Further studies were outlined to investigate which preparation steps and HMO support combinations were critical to producing the strong NO adsorbing material. These studies were also intended to provide a fundamental explanation for catalyst/adsorber performance and the effect of specific gases in the exhaust gas environment on NO adsorption.

HMO-Supported Gold and Silver Catalysts

<u>Evaluation of Bulk Au/HTO and Au/HTO:Si</u>

A single batch of 1.2% Au/HTO:Si was prepared, pretreated via a standard calcination, and tested at 20k/h (#211). Although significant efforts were made to fully acidify this

material, the residual Na^+ content of this material was rather high (1.38 wt.% Na^+, see Table 2). While CO and propylene oxidation behavior was satisfactory (100% and 82% conversion, respectively), maximum NOx conversion was only 13% at 309°C. A single batch of 1.16% Au/HTO was also prepared, pretreated via a standard calcination, and tested at 20k/h (#243 and #246). This sample also performed poorly, with overall results very similar to the Au/HTO:Si sample.

Evaluation of Bulk Ag/HTO and Ag/HTO:Si

A single Ag/HTO:Si batch containing 4.5 wt.% Ag was evaluated along with two Ag/HTO batches containing 4.0% and 4.2% Ag. The selection of Ag as a potentially active catalyst for screening purposes was largely based on results obtained independently by both LLNL and Ford Motor Co. The results obtained for the Ag/HTO:Si batch at 20 k/h (#199) were unimpressive; the maximum NOx conversion was very low (12% at 504°C). The overall oxidation activity of this material was very similar to that of the acidified H^+/HTO:Si support material (see Figure 14 below and Figure 10). Note that only the propylene showed any significant reactivity at 500°C. X-ray diffraction results for the calcined material indicated the presence of only weakly crystalline anatase.

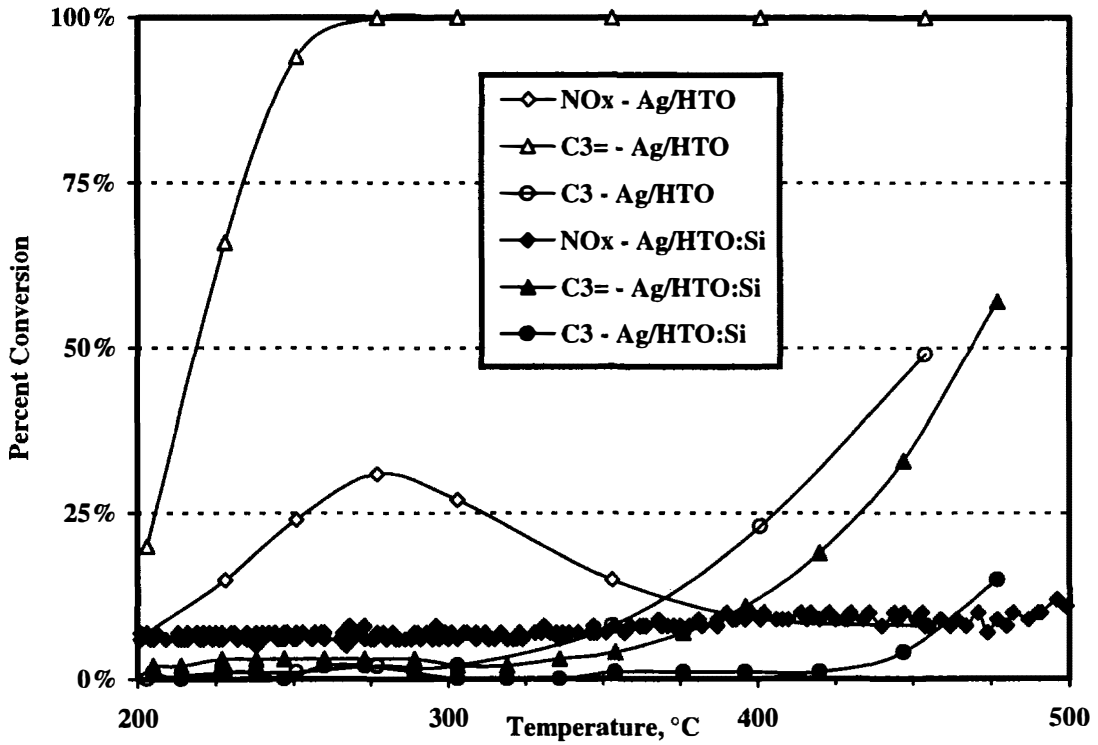

Figure 14. Comparison Ag/HTO (isothermal profile) and Ag/HTO:Si ("ramp-down" profile) powders at 20,000 1/h.

A 4.0% Ag/HTO material was prepared, pretreated via a calcination at 600°C, and run isothermally at 20 k/h (#226). This sample had a maximum NOx conversion of 31% at 277°C; at 277°C, the oxidation of CO and propylene was essentially 100%, while propane oxidation did not light-off until 300°C (see Figure 14). Thus, in contrast to the

Ag/HTO:Si material, the Ag/HTO material was relatively active for NOx reduction activity. Use of the HTO rather than the HTO:Si support resulted in a significant enhancement of the oxidation activity for Ag/HTO catalyst. X-ray diffraction analysis of the calcined Ag/HTO material showed the presence of fairly crystalline anatase. As in the case of the Ag/HTO:Si catalyst, these x-ray results for the as-calcined samples gave no indication of the nature of the Ag phases present. The only difference observed was the increase in crystallinity of the anatase present in the case of the Ag/HTO catalyst. Both the Ag/HTO and Ag/HTO:Si systems were identified for continued development so as to understand the role of support chemistry (presence of Si), Ag loading, and pretreatment/reaction conditions in determining catalyst performance.

HMO-Supported Noble Metal Catalysts

Evaluation of Bulk Rh/HTO:Si

Two batches of Rh/HTO:Si were prepared. The first batch consisted of a 1.15% Rh/HTO:Si catalyst which containing a higher than expected Na loading (1.33% Na^+) given the acidification treatment used during batch preparation. This material was tested at 20 k/h (#20), achieving a maximum NOx conversion of only 5% at 473°C (similar to the performance of the H^+/HTO:Si support material). Oxidation activity at 473°C for this material was good (100% CO, 100% propylene, and 20% propane conversion), slightly better than that observed for the H^+/HTO:Si support material. X-ray diffraction results for this sample in calcined form revealed only the existence of weakly crystalline anatase.

Because of a concern that the slightly elevated Na^+ level in this batch may have been detrimental to catalyst performance, a second 1.02% Rh/HTO:Si batch was synthesized with a lower Na concentration (0.09% Na, see Table 2). This material was tested after pretreatment using both the calcination only and the reduction + calcination procedures. Comparing both Rh/HTO:Si catalysts after the calcination only (600°C) pretreatment, the lower Na^+ batch performed slightly better at 20 k/h (#27) than the higher Na^+ batch, having a slightly higher maximum NOx conversion at a lower temperature (14% at 342°C). For this lower Na Rh/HTO:Si material, no difference in catalyst performance was observed in the case of the reduction + calcination pretreatment (#38) vs. the calcination only pretreatment.

Evaluation of Bulk Pd/HTO:Si and Pd/HZO:Si

Two Pd/HTO:Si and one Pd/HZO:Si materials were prepared and tested at 20 k/h. The two Pd/HTO:Si materials were prepared using different Pd precursors (see Table 2) and evaluated after a pretreatment procedure consisting of calcination at 600°C. For the Pd/HTO:Si material prepared using an acidic (HNO_3/HCl) Pd solution, the maximum NOx conversion was 23% at 188°C (#18). The oxidation behavior was especially good considering the low temperature (188°C); 100%, 82%, and 1% conversions for CO, propylene, and propane, respectively. X-ray diffraction results showed that this calcined Pd/HTO:Si material contained both PdO and weakly crystalline anatase.

For the second Pd/HTO:Si material prepared from a 10% Pd ammine solution, the maximum NOx conversion was 30% at 198°C (#58). The oxidation of CO, propylene, and propane was similar as in the case with the previous Pd/HTO:Si material. Worthy of note, however, is the fact the Pd/HTO:Si material prepared using the acidic Pd precursor resulted in a significantly lower residual Na^+ content (0.27 vs. 1.80 wt.% Na^+, see Table 2). Since the catalyst activity results for these two Pd/HTO:Si materials were so similar, it is not apparent that this difference in Na^+ content played a significant role in catalyst performance.

A 0.87% Pd/HZO:Si was prepared using the acidic Pd precursor and evaluated after pretreatment via 600°C calcination (#37). The maximum NOx conversion was 26% at 220°C, similar to the Pd/HTO:Si results except for a shift to a slightly higher temperature. The oxidation behavior of this catalyst was nearly identical to that of the Pd/HTO:Si catalysts.

Evaluation of Bulk Pt/HTO:Si and Pt/HZO:Si

A 1.19% Pt/HTO:Si material was evaluated at 20 k/h (#17) and 50 k/h (#19); the maximum NOx conversions were 88% at 188°C (Figure 15) and 73% at 247°C, respectively. Oxidation of CO and propylene was outstanding over this catalyst, exhibiting 100% conversion for both reactions at either space velocity at the maximum NOx conversion temperature. However, propane conversion was minimal (2-3%) for either test condition at the maximum NOx conversion temperature.

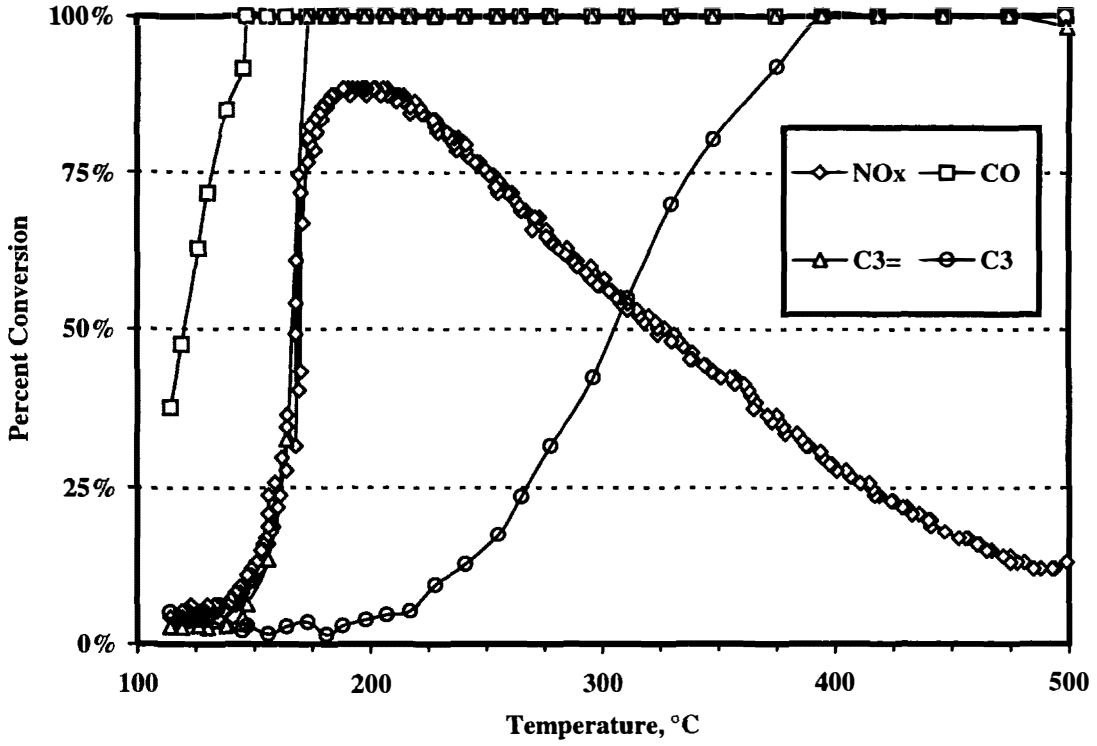

Figure 15. Activity of Pt/HTO:Si powder at 20,000 1/h.

X-ray diffraction results showed that this catalyst consisted of a mixture of metallic Pt (minor phase) and weakly crystalline anatase/brookite (major phase).

A 0.77% Pt/HZO:Si material was evaluated at 20 k/h (#60); the maximum NOx conversion was significantly lower, 31% at 227°C (Figure 16). The oxidation activity of this material was nearly identical to the Pt/HTO:Si catalyst. Although the maximum NOx conversion for this catalyst was significantly lower than that observed for the Pt/HTO:Si catalyst, the overall oxidation activity of the two catalysts was nearly identical. Considering this initial screening data, there was preliminary evidence for the HTO:Si support being somewhat more active than the HZO:Si support. However, due to the significant difference in Pt loading between the two samples and the reasonable activity of the Pt/HZO:Si catalyst, both Pt/HTO:Si and Pt/HZO:Si materials were identified as candidates for further studies.

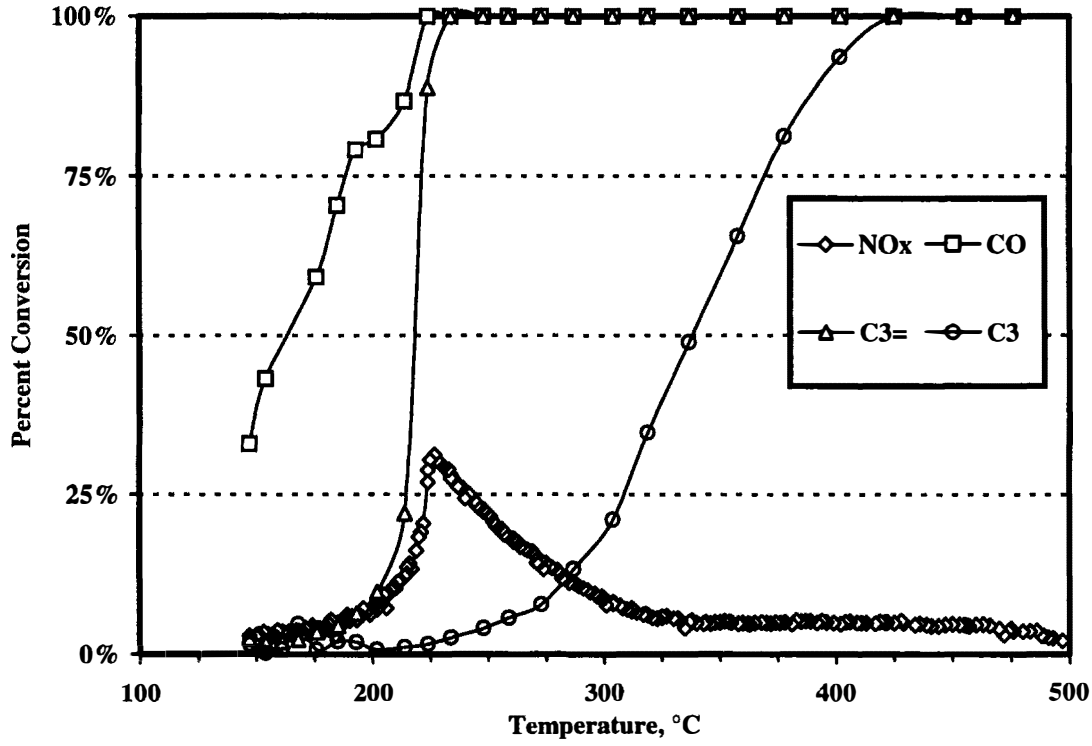

Figure 16. Activity of Pt/HZO:Si powder at 20,000 1/h.

Discussion of Results

The base HMO supports (HTO, HTO:Si, HZO, HZO:Si) had little NOx reduction activity for temperatures less than 450°C. The metals on the HMO supports that significantly improved NOx reduction activity were Pt, Pd, and Ag. Not suprisingly, these elements are among those most likely to remain in a metallic state in the oxidizing environments typical of the calcination and reaction conditions used in this study. For specific support and pretreatment condition combinations, Cu was found to have unique NOx adsorbing characteristics. Although the NOx adsorption characteristics of bulk CuO are well recognized,[64] this supported Cu material provides a new option for NOx adsorbing applications.

Pt is a successful NOx reduction catalyst on both HTO:Si and HZO:Si supports. The 1.2% Pt/HTO:Si reduced 88% of the NOx while the 0.77% Pd/HZO:Si reduced only about 31% of the NOx at 20 k/h. Of additional significance, the temperature of maximum NOx reduction was 39°C lower for the Pt/HTO:Si catalyst. Additional tests would be required to determine whether the increased maximum NOx conversion or the lower temperature of maximum NOx conversion was caused by the increased Pt loading or the difference in the support chemistry. An additional benefit of the Pt/HTO:Si material was that the oxidation activity occurred ~25°C higher in temperature than for the Pt/HZO:Si material. Again, additional experiments would be required to determine whether the oxidation temperature shift was Pt loading or support chemistry related. The metallic state of the Pt particles supported on the HTO:Si support was confirmed by x-ray diffraction analysis.

While not quite as active as Pt, Pd on both HTO:Si and HZO:Si was found to be moderately active for NOx reduction. While the 1.3% Pd/HTO:Si material reduced only 31% of the NOx as compared to 88% for the 1.2% Pt/HTO:Si material, Pd is significantly less expensive. Therefore, on a costs basis, Pd might be more effective than Pt. Pd on either support resulted in significant oxidation of CO and propylene in the 200 to 220°C temperature range. Overall, little distinction was noted between the HTO:Si and the HZO:Si support materials. Since PdO was identified by x-ray diffraction after calcination, it is somewhat suprising that the Pd/HTO:Si catalysts exhibited appreciable NOx conversion. However, it is possible that the PdO phase itself was either mildly active for NOx reduction or easily reduced in the reaction environment.

The poor performance of the Rh/HTO:Si catalysts was surprising since supported-Rh catalysts are known to have excellent NOx reduction performance, particularly at typical three-way automotive catalyst operating conditions.[4,65] Our poor results obtained with the Rh/HTO:Si are probably indicative of Rh existing in an oxidized state (Rh_2O_3) after 600°C calcination of these samples.[66] In previous studies where careful pretreatment (e.g., calcination followed by reduction) has been used to ensure the presence of metallic Rh particles prior to reaction environment exposure, high NOx reduction activity was observed for supported Rh catalysts.[50]

A relatively high loading (~4%) of Ag on HTO was fairly active for NOx reduction (~33% maximum NOx conversion); however, the temperature of maximum NOx reduction (277°C to 303°C) was significantly higher than Pt or Pd by about 75°C. Depending on the design situation, the higher temperature activity could be an asset or a liability. In the range of the maximum NOx reduction temperature, Ag/HTO was a very good oxidation catalyst for CO and propylene. Ag/HTO:Si performed notable different than Ag/HTO, exhibiting very low NOx reduction activity and being only marginally better than H^+/HTO:Si for NOx reduction. The results for the Ag/HTO catalyst are not suprising since supported Ag catalysts have been previously shown by Ford Motor Company and LLNL to possess appreciable NOx reduction activity. The fact that Ag_2O, which forms at low temperatures in oxidizing environments, dissociates to Ag metal at temperatures above 230°C,[67] undoubtedly favors the existence of metallic Ag particles under calcination or reaction conditions used in our studies. The actual Ag phases present in the Ag/HTO or Ag/HTO:Si samples after calcination could not be identified by x-ray diffraction.

Cu on any of the HMO supports displayed little catalytic NOx reduction activity; however, Cu/HZO:Si was a strong NOx adsorber depending on pretreatment conditions. Determining the exact cause and effect relationship(s) between the support chemistry, Na^+ level, and pretreatment methods and the NOx adsorption capability of the resulting Cu/HZO:Si material was beyond the scope of this report.

Summary

In view of the results from this screening study, Pt/HTO:Si, Pt/HZO:Si, Pd/HTO:Si, Pd/HZO:Si and Ag/HTO were selected for further study. Based on the following three parameters, materials were ranked in terms of desirability for automotive application; maximum NOx conversion, the temperature at which maximum NOx conversion occurs, and the breadth of the NOx conversion peak as a function of temperature. The effect of material processing parameters, Na^+ content, and active metals concentration on these three parameters was discerned though a extensive series of materials preparation and catalyst activity evaluations. Based on these evaluations which will be described in a future report(s), a patent application was filed in July 1996 outlining the capabilities of the Pt/HMO, Pd/HMO, and combinations of PtPd/HMO materials.[68]

Cu was selected for a separate study as a NOx adsorbing material. The effect of alkali type, alkali concentration, Cu concentration, and support chemistry was discerned through a comprehensive series of material preparations and gas contacting experiments, which will be described in a future report. Based on these experiments, a patent application was filed in July 1996 outlining the capabilities of the Cu/HMO adsorbing material.[69]

Intentionally Left Blank

References

[1] T. J. Truex, R. A. Searles, and D. C. Sun, Plat. Met. Rev., **36**(1), 2 (1992).

[2] K. C. Taylor, Catal. Rev.-Sci. Eng., **35**(4), 457 (1993).

[3] C. K. Narula, J. E. Allison, D. R. Bauer, and H. S. Gandhi, Chem. Mater., **8**, 984 (1996)

[4] K. C. Taylor, in Catalysis Science and Technology, Vol. 5, J. R. Anderson and M. Boudart, eds., Springer-Verlag, Berlin, 119 (1984).

[5] R. G. Dosch, T. J. Headley, and P. Hlava, J. Am. Ceram. Soc. **67**, 354 (1984).

[6] A. Clearfield, Ind. Eng. Chem. Res. **34**, 2865 (1995).

[7] H. P. Stephens, R. G. Dosch, and F. V. Stohl, Ind. Eng. Chem. Res. Devel. **24**, 15 (1985).

[8] H. P. Stephens and R. G. Dosch, Stud. Surf. Sci. Catal. **31**, 271 (1987).

[9] R. G. Dosch, H. P. Stephens, and F. V. Stohl, Sandia Report, SAND89-2400, Sandia National Laboratories, Albuquerque, (1990).

[10] R. G. Dosch and L. I. McLaughlin, Sandia Report, SAND92-0388, Sandia National Laboratories, Albuquerque, (1992).

[11] S. E. Lott, T. J. Gardner, L. I. McLaughlin, and J. B. Oelfke, Accepted for Publication in Fuel.

[12] S. E. Lott, T. J. Gardner, L. I. McLaughlin, and J. B. Oelfke, Prep. Amer. Chem. Soc., Fuel Chem. Div., **39,** 1073 (1994).

[13] P. S. Peercy, R. G. Dosch, and B. Morosin, Sandia Report, SAND76-0556, Sandia National Laboratories, Albuquerque, (1977).

[14] R. G. Dosch, Sandia Report, SAND80-1212, Sandia National Laboratories, Albuquerque, (1981).

[15] R. G. Dosch, H. P. Stephens, F. V. Stohl, B. C. Bunker, and C. H. F. Peden, Sandia Report, SAND89-2399, Sandia National Laboratories, Albuquerque, (1990).

[16] T. J. Gardner and L. I. McLaughlin, in Mater. Res. Soc. Symp. Proc., to be published.

[17] C. J. Brinker and G. W. Scherer, Sol-Gel Science: The Physics and Chemistry of Sol-Gel Processing, Academic Press, San Diego, (1990).

[18] J. Livage, M. Henry, and C. Sanchez, Prog. Solid State Chem., **18**, 259 (1988).

[19] C. Sanchez, J. Livage, M. Henry, and C. Babonneau, J. Non-Cryst. Solids, **100**, 65 (1988).

[20] T. J. Boyle, T. L. Alam, and T. J. Gardner (unpublished work).

[21] W. H. Gitzen, Alumina as a Ceramic Material, American Ceramic Society, Columbus (1970).

[22] H. Arai, M. Machida, Appl. Catal. A, **138**, 161 (1996).

[23] T. J. Gardner, Ph.D. Thesis, University of New Mexico, 1994.

[24] R. D. Shannon, J. Appl. Phys., **35** 3414 (1964).

[25] R. D. Shannon and J. A. Pask, J. Am. Ceram. Soc., **48**, 391 (1965).

[26] Y. Iida and S. Ozaki, J. Am. Ceram. Soc., **44**, 120 (1961).

[27] J. R. Sohn, H. J. Jang, M. Y. Park, E. H. Park, and S. E. J. Park, Mol. Catal., **93**, 149 (1994).

[28] P. K. Doolin, S. Alerasool, D. J. Zalewski, and J. F. Hoffman, Catal. Lett., **25**, 209, (1994).
[29] Y. Suyama, and A. Kato, Yogyo-Kyokai-Shi, **86** (3), 119 (1978).
[30] C. U. I. Odenbrand, S. L. T. Andersson, L. A. H. Andersson, J. G. M. Brandin, and G. Busca, J. Catal., **125**, 541 (1990).
[31] K. L. Walther, A. Wokaun, B. E. Handy, and A. Baiker, J. Non-Cryst. Solids, **134**, 47 (1991).
[32] P. J. Dirken, M. E. Smith, and H. J. Whitfield, J. Phys. Chem., **99**, 395 (1995).
[33] M. Aizawa, Y. Nosaka, and N. Fujii, J. Non-Cryst. Solids, **128**, 77 (1991).
[34] J. B. Miller and E. I. Ko, J. Catal., **159**, 58 (1996).
[35] R. C. DeVries, R. Roy, and E. F. Osborn, Trans. Brit. Ceram. Soc.,**53**, 533 (1954).
[36] I. M. Miranda Salvado and J. M. Fernandez Navarro, J. Non-Cryst. Solids, **147-148**, 256 (1992).
[37] C.-H. Hung and J. L. Katz, J. Mater. Res., **7**, 1861 (1992).
[38] M. K. Akhtar, S. E. Pratsinis, and S. V. R. Mastrangelo, J. Am. Ceram. Soc., **75**, 3408 (1992).
[39] S. Vemury and S. E. Pratsinis, J. Am. Ceram. Soc., **78**, 2984 (1995).
[40] Z. Liu and R. J. Davis, J. Phys. Chem., **98**, 1253 (1994).
[41] A. Y. Stakheev, E. S. Shpiro, and J, Apijok, J. Phys. Chem., **97**, 5668 (1993).
[42] R. B. Greegor, F. W. Lytle, D. R. Sandstrom, J. Wong, and P. Schultz, J. Non-Cryst. Solids, **55**, 27 (1983).
[43] C. E. Curtis and H. G. Sowman, J. Am. Ceram. Soc., **36**, 198 (1953).
[44] R. C. Garvie, J. Phys. Chem., **69**, 1238 (1965).
[45] K. S. Mazdiyasni, C. T. Lynch, and J. S. Smith, J. Am. Ceram. Soc., **49**, 286 (1966).
[46] H. J. M. Bosman, E. C. Kruissink, J. van der Spoel, and F. van den Brink, J. Catal., **148**, 660 (1994).
[47] W. Held, A. Konig, T. Richter, and L. Ruppe, SAE Technical Paper No. 900496 (1990).
[48] M. Iwamoto and H. Hamada, Catal. Today, **10**, 57 (1991).
[49] M. Iwamoto, N. Mizuno, and H. Yahiro, in Proceedings of the 10th International Congress on Catalysis, L. Guczi, F. Solymosi, and P. Tetenyi, eds., Elsevier, Amsterdam, 1285 (1993).
[50] A. Obuchi, A. Ohi, M. Nakamura, A. Ogata, K. Mizuno, and H. Ohuchi, Appl. Catal. B, **2**, 71 (1993).
[51] C. F. Baes and R. E. Mesmer, The Hydrolysis of Cations, John Wiley and Sons, New York (1976).
[52] D. R. Monroe, C. L. Dimaggio, D. D. Beck, and F. A. Matekunos, SAE Technical Paper No. 930737 (1993).
[53] K. C. C. Kharas, H. J. Robota, and D.-J. Liu, Appl. Catal. B, **2**, 225 (1993).
[54] H.-W. Jen, C. Montreuil, and H. Gandhi, Prepr. Am. Chem. Soc., Fuel Chem. Div., **40**[4],1056 (1995).
[55] K. C. C. Kharas, H. J. Robota, D.-J. Liu, and A. K. Datye, Prepr. Am. Chem. Soc., Fuel Chem. Div., **40**[4],1068 (1995).
[56] D. Monroe, C. L. DiMaggio, "Evaluation of a Copper/Zeolite Catalyst to Remove

Nitrogen Oxides from Lean Exhaust," Report GMR-7799 (1992).
[57] K. C. C. Kharas, H. J. Robota, and A. Datye, in Environmental Catalysts ed. By J. Armor, American Chemical Society, Washington, p39 (1994).
[58] K. Otto, J. M. Andino, and C. L. Parks, J. Catal., **131**, 243 (1991).
[59] L. M. Carballo and E. E. Wolf, J. Catal., **53**, 366 (1978).
[60] T. Engel and G. Ertl, Adv. Catal., 28, 2 (1979).
[61] H. K. Shin, H. Hirabayashi, H. Yahiro, M. Watanabe, M. Iwamoto, Catal. Today, **26**, 13 (1995).
[62] C. Contescu, V. T. Popa, J. B. Miller, E. I. Ko, and J. A. Schwarz, J. Catal., **157**, 244 (1995).
[63] H. H. Kung and M. C. Kung, Catal. Today, **30**, 5 (1996).
[64] H. S. Gandhi and M. S. Shelef, J. Catal., **28**, 1 (1973).
[65] M. Shelef and G. W. Graham, Catal. Rev.-Sci. Eng., **36**, 433 (1994).
[66] J. Barbier and D. Duprez, Appl. Catal. B, **4**, 105 (1994).
[67] CRC Handbook of Chemistry and Physics, R. C. Weast, ed., CRC Press, Boca Raton (1983).
[68] T. J. Gardner, S. E. Lott, S. J. Lockwood, and L. I . McLaughlin, Material and System for Catalytic Reduction of Nitrogen Oxide in an Exhaust Stream of a Combustion Process, U. S. Patent Application, Filed July, 1996.
[69] S. E. Lott, T. J. Gardner, L. I . McLaughlin, J. B. Oelfke, and C. A. Matlock, Nitrogen Oxide Absorbing Material, U.S. Patent Application, Filed July, 1996.

Intentionally Left Blank

Appendix 1 - Listing of Catalyst Activity Results

			SV	Temp	Conversion				
Run	LEP #	Catalyst	1/h	C	NOx	CO	propylene	propane	Remarks
Homogeneous Gas Phase Reactions									
187	none	open quartz tube	50000	502	8%	-15%	14%	23%	
188	none	HTO:Si on Cordierite	50000	503	6%	-4%	15%	7%	
189	none	HTO:Si on Cordierite	50000	503	6%	-5%	12%	7%	repeat of run 188 with same monolith
190	none	HTO:Si on Cordierite	50000	502	6%	-4%	13%	9%	repeat of run 190 with same monolith with NO2 feed
191	none	HTO:Si on Cordierite	50000	503	6%	-8%	9%	6%	repeat of run 191 with same monolith with NO2 feed
Bulk Washcoat Powders Supplied by General Motors									
89	none	DSZ-5b Washcoat	20000	480	24%	76%	100%	76%	
91	none	DSZ-5b Washcoat	20000	475	25%	80%	100%	81%	re-run of run 89 sample
90	none	Tech-3 Washcoat	20000	171	63%	100%	100%	1%	
Cordierite Monolith-Supported Catalysts from GM and Commercial Catalyst Suppliers									
47	none	DSZ-5b Monolith	20000	504	29%	-231%	92%	66%	run without steam
48	none	DSZ-5b Monolith	20000	503	12%	-197%	95%	29%	run with steam
4	none	Tech-3 Monolith	20000	169	74%	100%	100%	4%	
2	none	Tech-3 Monolith	50000	190	48%	100%	100%	0%	
240	none	JM CuZSM-5 Washcoat	50000	575	57%	85%	100%	100%	as received, no water, isothermal
239	none	JM CuZSM-5 Washcoat	50000	575	52%	45%	100%	100%	as received, with water, isothermal
238	none	JM CuZSM-5 Washcoat	50000	575	61%	23%	100%	72%	calcined, no water, isothermal
237	none	JM CuZSM-5 Washcoat	50000	554	69%	-23%	97%	100%	calcined, with water, isothermal
309	none	JM CuZSM-5 Washcoat	50000	568	9%	-160%	93%	100%	sweep run after 1 week streaming with air at 7%water/650C
232	none	PtZSM-5	50000	317	45%	100%	100%	15%	as received, no water
233	none	PtZSM-5	50000	294	54%	100%	100%	18%	as received, with water
236	none	PtZSM-5	50000	267	46%	100%	100%	11%	calcined, no water
235	none	PtZSM-5	50000	257	37%	100%	100%	2%	calcined, with water
262	none	PtZSM-5	50000	379	28%	100%	100%	17%	sweep run after 1 week streaming with air at 7%water/650C
298	none	PtZSM-5	50000	380	28%	100%	100%	10%	sweep run after 1 week streaming with air at 7%water/650C

Bulk H^+/HTO:Si and H^+/HZO:Si Powder									
9	1-24C	H/HTO:Si Powder	20000	502	16%	-48%	76%	24%	0.05% Na, pH=2.6, maximum acidification
6	1-24C	H/HTO:Si Powder	50000	500	10%	-23%	56%	10%	0.05% Na, pH=2.6, maximum acidification
11	1-23C	H/HZO:Si Powder	20000	479	4%	73%	100%	20%	0.05% Na, pH=2.6, maximum acidification
7	1-23C	H/HZO:Si Powder	50000	501	2%	38%	92%	10%	0.03% Na pH=2.6, maximum acidification
Bulk Co/HTO:Si and Co/HZO:Si									
13	1-21C	2.07% Co/HTO:Si	20000	500	5%	12%	94%	22%	
56	1-21RC	2.07% Co/HTO:Si	20000	378	5%	81%	88%	4%	reduced prior to calcination, 0.25% Na
8	1-21C	2.07% Co/HTO:Si	50000	506	3%	-62%	42%	4%	
15	1-29C	2.71% Co/HZO:Si	20000	432	13%	-47%	81%	30%	
Bulk Ni/HZO:Si									
57	1-70RC	2.32% Ni/HZO:Si	20000	367	4%	75%	70%	6%	0.29% Na, reduced prior to calcination
Bulk Cu/HTO:Si, Cu/HZO, and Cu/HZO:Si									
12	1-22C	2.97% Cu/HTO:Si	20000	254	10%	59%	93%	2%	0.07% Na
14	1-22C	2.97% Cu/HTO:Si	50000	272	6%	20%	63%	2%	0.07% Na
33	1-48-1C	2.25% Cu/HZO	20000	393	14%	100%	100%	100%	0.12% Na
43	1-48-2RC	2.25% Cu/HZO	20000	368	12%	100%	100%	100%	0.12% Na, reduced prior to calcination
51	1-66RC	2.14% Cu/HZO	20000	378	17%	100%	100%	100%	0.04% Na, repeat prep of 1-48-1RC, reduced prior to calcination
34	1-47-1C	2.41% Cu/HZO:Si	20000	307	15%	100%	96%	2%	0.14% Na
45	1-47-2RC	2.41% Cu/HZO:Si	20000	500	92%	76%	49%	9%	Na & K contaminated
50	1-47-2RC	2.41% Cu/HZO:Si	20000	465	40%	42%	36%	30%	re-run of Run 45 sample
Bulk Au/HTO, Au/HTO:Si, Ag/HTO, Ag/HTO:Si									
243	2-59C	1.16% Au/HTO	20000	503	12%	99%	69%	19%	0.76% Na, moderate NOx adsorption
246	2-59C	1.16% Au/HTO	20000	503	14%	98%	63%	18%	isothermal run with same sample from run 243
211	2-52-2C	1.2% Au/HTO:Si	20000	309	13%	100%	82%	2%	1.38% Na, high NOx adsorption
226	2-54-1C	4.0% Ag/HTO	20000	277	31%	100%	100%	2%	0.05% Na
283	2-73-2C	4.23% Ag/HTO	20000	303	33%	100%	100%	2%	isothermal run, 0.04%Na
199	2-46-1C	4.5% Ag/HTO:Si	20000	504	12%	-8%	70%	38%	0.73% Na
Bulk Rh/HTO:Si									
20	1-32C	1.15% Rh/HTO:Si	20000	473	5%	100%	100%	20%	1.33% Na
27	1-41-1C	1.02% Rh/HTO:Si	20000	342	14%	100%	100%	2%	0.09% Na

38	1-41-2RC	1.02% Rh/HTO:Si	20000	359	14%	100%	100%	1%	0.09% Na, reduced and then calcined
22	1-32C	1.15% Rh/HTO:Si	50000	215	19%	100%	89%	1%	1.33% Na
Bulk Pd/HTO:Si and Pd/HZO:Si									
18	1-31C	1.31% Pd/HTO:Si	20000	188	23%	100%	82%	1%	0.27% Na, Pd from Pd dissolved in HCl/HNO_3
58	1-61-2C	1.06% Pd/HTO:Si	20000	198	30%	100%	100%	0%	0.56% Na, Pd from Pd tetraammine nitrate
37	1-52C	0.87% Pd/HZO:Si	20000	220	26%	100%	100%	-2%	0.13% Na, Pd from Pd dissolved in HCl/HNO_3
Bulk Pt/HTO:Si and Pt/HZO:Si									
17	1-30C	1.19% Pt/HTO:Si	20000	188	88%	100%	100%	3%	0.20% Na
19	1-30C	1.19% Pt/HTO:Si	50000	247	73%	100%	100%	2%	0.20% Na
60	1-64-2C	0.77% Pt/HZO:Si	20000	227	31%	100%	100%	2%	0.11% Na

Intentionally Left Blank

Distribution:

Kathleen Taylor, Department Head
Physics and Physical Chemistry Department
Research and Development Center
General Motors Corporation
Building 1-18
30500 Mound Road
Box 9055
Warren, MI 48090-9055

Haren S. Gandhi
Technical Fellow
Manager, Chemical Engineering Department
Scientific Research Laboratories, MD-3179
Ford Research Laboratory
20000 Rotunda Drive
Dearborn, MI 48121-2053

Michael Brady
Chrysler Corporation, CIM 482-01-19
800 Chrysler Drive East
Auburn Hills, MI 48326-2757

Michael J. Royce
Chrysler Corporation, CIM 482-01-07
800 Chrysler Drive East
Auburn Hills, MI 48326-2757

Sandia Internal:

MS 0706 S. E. Lott, 6113 (10)
MS 0709 T. J. Gardner, 6113 (10)
MS 0709 L. I. McLaughlin, 6113
MS 0959 S. J. Lockwood, 1492
MS 9018 Central Technical Files, 8523-2
MS 0899 Technical Library, 4414 (5)
MS 0619 Review and Approval Desk, 12630 for DOE/OSTI (2)
MS 0161 Patent and Licensing Office, 11500 (3)

Intentionally Left Blank